International Journal of Applied Mathematics

Volume 39 No. 1s 2026,

ISSN: 1311-1728 (printed version); ISSN: 1314-8060 (on-line version)

BRE-CAD: AN IOT-ENABLED DEEP LEARNING FRAMEWORK FOR MAMMOGRAPHIC BREAST CANCER DETECTION AND CLINICAL DECISION SUPPORT

Yazeed Meshal Alshurbi[1], Labib M. Labib[1], Sarah M. Ayyad[1,2,*]

[1] Computers and Control Systems Department, Faculty of Engineering, Mansoura University, Mansoura, 35516, Egypt

[2]Faculty of Engineering, Mansoura National University, Gamasa, 35712, Egypt

Abstract

Breast cancer remains one of the leading causes of cancer-related mortality among women worldwide, highlighting the urgent need for reliable computer-aided diagnosis (CAD) systems that support early screening and clinical decision-making. This paper presents BRE-CAD, an end-to-end IoT-enabled CAD framework for breast cancer detection that integrates mammographic data preprocessing, deep learning–based lesion localization, graphical clinical visualization, and database-driven diagnostic management. The proposed methodology follows a structured pipeline comprising dataset curation and annotation, model training and optimization, system integration, and longitudinal data storage. A curated subset of 5,304 mammographic images (1,768 malignant and 3,536 benign) extracted from the VinDr-Mammo dataset was processed through a dedicated data pipeline involving mass extraction, bounding box annotation, and partitioning into training (80%), validation (15%), and testing (5%) subsets. A Faster R-CNN detection model was employed to simultaneously localize suspicious regions and classify breast lesions. The trained model was embedded into a graphical user interface and connected to a PostgreSQL backend through an IoT-based architecture, enabling real-time and offline diagnostic visualization as well as secure storage of clinical records. Experimental results demonstrate stable training convergence, with validation performance achieving a recall of 0.71, precision of 0.64, and F1-score of 0.67. Image-level evaluation yielded 309 true-positive cancer detections and 735 true-negative healthy classifications. In addition to quantitative metrics, qualitative analysis conducted on a randomly selected 5% test subset confirmed reliable lesion localization, effective suppression of false detections in normal mammograms, and conservative flagging of ambiguous cases. Although the achieved performance remains moderate compared to fully supervised high-resolution benchmark systems, BRE-CAD exhibits clinically desirable recall-oriented behavior and interpretable detection outcomes. By integrating deep learning inference with IoT-based data management and clinician-in-the-loop visualization, the proposed framework provides a practical screening-oriented decision-support system aimed at assisting radiologists rather than replacing expert judgment.

Keywords: Breast Cancer; Deep Learning; IoT; Computer-aided diagnosis; Mammography

Received: Sep 17 2025

International Journal of Applied Mathematics

Volume 39 No. 1s 2026,

ISSN: 1311-1728 (printed version); ISSN: 1314-8060 (on-line version)

1. Introduction

Breast Cancer (BC) is a health issue that is most commonly diagnosed in women across the globe and that has been a huge health problem to the population. In 2022, it was estimated that the world had some 2.3 million new cases and 670,000 deaths [1], [2], [3]. It is a disease that is found in almost all countries: BC was by far the most prevalent cancer in women in 157 of 185 countries in 2022, which highlights its universal presence in all countries [4]. Although the incidence has been the highest in more developed areas, mortality is usually disproportionately greater in less-developed areas. As an illustration, the largest age-standardized incidence percentages are in Australia/New Zealand (95.5%), Western Europe (90.7%) and Northern America (89.4%). By comparison, South-Central Asia (26.2%), Middle and Eastern Africa (33%) and Central America (39.5%) have significantly lower incidence percentage [5], [6]. Various countries with low rates of incidence in the past are rapidly increasing at a rate of 3-5 per annum of new infections worldwide [7]. Such geographic differences demonstrate the differences in detection, screening programs, awareness, and treatment accessibility. Several risk factors of BC are known: some are non-modifiable, including advancing age, female sex, hereditary genetic mutations, and some factors are modifiable and include obesity, alcohol use, lack of physical exercises, and reproductive history [8], [9]. Other factors which contribute are the environmental factors and previous exposure to radiation. Since in most cases women get BC without explicit risk factors, screening and early detection are crucial in minimizing the burden of the disease. In addition to health, BC presents a large burden to the society due to the decreased life expectancy, high healthcare expenses and the emotional and economic stress it causes to the families [10]. It also has some effects on national productivity because women who are at their most prolific working and care giving age can be placed on long treatment periods, less work capacity or die prematurely all of which weaken the work force and adds strain on the health care and social support frameworks [11], [12].

Scientists across the world have in turn responded by putting a lot of effort in coming up with sophisticated diagnostic tools, and early warning systems. As an example, BRCA1 and BRCA2 genetic testing can identify high-risk individuals prior to the onset of cancer [13], [14], [15], which will make it possible to prevent these cancers. The study of biomarkers has resulted in the identification of circulating tumor cells and cell-free DNA in blood [16], [17], [18], and they can be used as minimally invasive early-detection procedures. The sensitivity of early-stage detection is enhanced with the help of advances in medical imaging, including digital breast tomosynthesis (3D mammography), contrast-enhanced Magnetic Resonance Imaging (MRI), and ultrasound elastography [19], [20], [21], [22], [23]. Artificial intelligence (AI) and Deep Learning (DL) models have been used more recently in mammography, ultrasound and MRI to provide lesion detection, risk stratification, and early warning prediction with high accuracy [24], [25], [26], [27], [28]. These inventions emphasize the international scientific interest to lower the mortality of BC by diagnosing the disease at the earliest and most preventable stage.

Received: Sep 17 2025

International Journal of Applied Mathematics

Volume 39 No. 1s 2026,

ISSN: 1311-1728 (printed version); ISSN: 1314-8060 (on-line version)

Computer-Aided Diagnosis (CAD) systems are computational frameworks designed to assist clinicians in the interpretation of medical images by automatically analyzing imaging data and highlighting suspicious findings. A typical CAD system consists of several stages, including image preprocessing, feature extraction, lesion detection or segmentation, classification, and result visualization. Rather than replacing physicians, CAD systems function as decision-support tools that enhance diagnostic consistency, reduce human error, and improve early disease detection rates. In the context of breast cancer, CAD systems play a particularly critical role due to the subtle and heterogeneous appearance of lesions in mammographic images. Early-stage tumors may present as low-contrast masses or microcalcifications that are difficult to detect, even for experienced radiologists. Therefore, integrating CAD systems into breast imaging workflows can improve sensitivity, assist in prioritizing high-risk cases, and support large-scale screening programs where radiologist workload is substantial. Studies of CAD systems are several decades old as helping systems to support radiologists in recognizing and categorizing breast lesions. Initial methods of CAD were hand-based models, in which the features of images (texture, shape, and statistical values) were manually obtained and categorized with algorithms such as Support Vector Machines (SVM) or k-Nearest Neighbors (kNN). Although these methods were able to give an early breakthrough, they were usually limited in accuracy and generalization as features that were manually created could not perfectly represent the fluctuating appearance of tumors in mammographies. The dominant tendency has been the introduction of deep learning, specifically, convolutional neural networks (CNNs), which allowed automated feature extraction, as well as directly learning a task through raw images. This development achieved a great level of detection and classification performance, and CNN-based systems became a trend in the research of BC CAD.

Over the past two decades, extensive research efforts have been dedicated to developing computer-aided diagnosis systems for breast cancer detection. These studies can broadly be categorized into two major paradigms: traditional machine learning approaches relying on hand-crafted feature extraction, and modern deep learning–based frameworks that learn discriminative representations directly from medical images. This section provides a structured overview of both paradigms, highlighting their evolution, strengths, and limitations, before discussing recent advances in deep learning–based breast cancer detection systems. Early breast cancer CAD systems were primarily based on conventional machine learning techniques combined with manually engineered image features. In these approaches, radiological characteristics such as texture descriptors, shape metrics, intensity statistics, and morphological features were extracted from mammographic regions of interest. These hand-crafted features were then classified using traditional algorithms such as Support Vector Machines (SVM), k-Nearest Neighbors (kNN), Random Forests, and Logistic Regression [29], [30], [31]. Although these methods demonstrated initial success in differentiating benign from malignant lesions, their performance was highly dependent on the quality and completeness of manually designed features. Moreover, handcrafted representations often failed to capture the complex and heterogeneous visual patterns of breast tumors, leading to limited generalization across datasets

Received: Sep 17 2025

Volume 39 No. 1s 2026,

ISSN: 1311-1728 (printed version); ISSN: 1314-8060 (on-line version)

and imaging conditions. As a result, these systems exhibited constrained robustness, particularly when dealing with low-contrast lesions, dense breast tissue, or variations in acquisition protocols.

in recent years, it has improved even further with more sophisticated detection models including Faster Region-based Convolutional Neural Network (R-CNN) [32], [33], [34], [35], [36] and You Only Look Once (YOLO) [37], [38], [39], [40]. these architectures integrate both detection and classification into a single system enabling the localization of suspicious regions and classification of benign and malignant lesions in real-time. In addition to these, a number of CNN architectures have been popular among BC CAD studies. The first models to be used included AlexNet [41], [42], [43], VGG16/VGG19 [41], [44], [45], [46], and GoogLeNet (Inception) [47], [48], [49], [50], [51], and their results showed that deep feature extraction has the potential to outperform traditional hand-crafted features. The more recent literature has made use of ResNet [52], [53], [54], [55], [56] and its more residual versions, which overcome the vanishing gradient issues and reach a better performance in classification. Also, DenseNet [57], [58], [59], [60], [61] has been investigated because of its effective reuse of features and good performance using a small amount of training data. Simultaneously, Inception-ResNet hybrids [48], [53], [56], [62], [63], MobileNet [64], [65], [66], [67], and EfficientNet [68], [69], [70] have been tested in terms of the lightweight but accurate implementation that can be used in real-time diagnosis. In addition to CNNs, some other deep learning methods have also been proposed. Sequential analysis of imaging slices with Recurrent Neural Networks (RNNs) and their gated counterparts, e.g. Long Short-Term Memory (LSTM) [71], [72], [73], [74], [75] and Gated Recurrent Units (GRU) [76], [77], [78], [79], [80], etc., have also been used, especially in dynamic contrast-enhanced MRI, where time is a factor. Besides these, research has investigated Bidirectional RNNs (Bi-RNNs) [81], [82], [83], that process input sequences both forward and backward, and thus more contextual dependencies between sequences of images. Two-way LSTMs (Bi-LSTMs) and two-way GRUs (Bi-GRUs) [84] are also reported in the literature, which enhance results in the temporal lesion characterization and risk prediction. Hybrid architectures have also used RNNs together with CNNs, with CNNs used to extract the spatial aspect and RNNs the temporal or sequential aspect, which has also led to superior results in multi-slice or longitudinal imaging data [85], [86], [87], [88], [89]. Regarding the imaging modalities, majority of the CAD research has concentrated on mammography which is the world standard of screening BC. The deep learning models trained on mammograms have demonstrated great improvement in sensitivity that detects microcalcifications and masses [90], [91], [92], [93], [94], [95]. Other modalities have also been explored: ultrasound imaging has been studied as a complementary tool [96], [97], [98], [99], especially effective in dense breast tissues, while MRI has been used in high-risk screening due to its superior sensitivity [100], [101], [102], [103], [104], [105]. Most recently, it has been suggested that multimodal strategies based on mammography, ultrasound, and MRI results can be used to resolve a certain degree of robustness and false positives [106], [107], [108], [109]. Even with those achievements, most of the published works still consider algorithmic benchmarks like

Received: Sep 17 2025

Volume 39 No. 1s 2026,

ISSN: 1311-1728 (printed version); ISSN: 1314-8060 (on-line version)

accuracy, sensitivity, specificity, area under the curve (AUC), and F1-scores as the primary metrics of evaluation [110], [111], [112].

An in-depth analysis of the existing literature as outlined in Table 1 reveals a number of critical gaps between the research on algorithms and its application in clinical settings in the use of BC CAD systems. In spite of the fact that the reviewed studies show excellent results in terms of its usage of a large range of AI models (R-CNN, YOLO, VGG, ResNet, DenseNet, Inception, EfficientNet, GRU/LSTM, and ViTs), the vast majority of them end at reporting the performance of the algorithm in terms of its accuracy, sensitivity, specificity, or F1-scores. Very little literature [30], [34] specifically talks of the development of a CAD system, and most of the literature is restricted to experiment models. This shows that there is a clear disparity between high accuracy in a research setting, and the application of these models to clinical applications. No one mentioned the use of relational databases including PostgreSQL, or similar to organize the diagnostic outputs. Such lack of data persistence and traceability is a serious obstacle to real-life application in clinical processes. The development of post-review software, almost all the studies do not answer the question of how the results may be reviewed once they are initially diagnosed, audited over time, and utilized in the follow-up consultations. There was little to no inclusion of such tools as GUIs, post-data visualization dashboards, or feedback loops. This exclusion makes the clinical usability and interpretability of any AI model even more accurate less useful.

In order to fill the research gaps, this paper introduces the BREAST-CAD system, which is a complete CAD system to detect and treat BC. The paper has made the following contributions: Database-based Diagnostic Record Management: we added the PostgreSQL structured database to store diagnostic data, annotations, and diagnostic metadata. This provides traceability, reproducibility, and long-term storage of the diagnostic outcomes and allows the clinicians to review previous cases, perform audits and provide multi-stage diagnosis. End-to-end Workflow Dataset Preparation and Annotation: This system has a powerful preprocessing pipeline consisting of dataset partitioning, bounding box annotation (code-based and manual), and error correction. This will ensure that the training data is of high-quality and also solve the problem of error in annotation that would otherwise lower model reliability. Comparative Assessment and Optimal Model: Faster R-CNN (Regional Convolutional Neural Network) was trained and assessed on partitioned datasets and several measures of performance (accuracy, precision, recall, F1-score, and AUC) were examined. The process of optimization was done through iterative reconfiguration and retraining to guarantee that the model deployed in the end is the best trade-off between accuracy and efficiency. Combination of AI Detection and Clinical Usability: we have created a complete CAD system with the Faster R-CNN detection model and a graphical interface. Such interface enables clinicians to see the areas of lesions, see the confidence scores, and actively confirm the outcome of detection in order to increase the interpretability and clinical decisions. Real Time and Offline Data Viewing: In addition to detection, the system has real-time and offline monitoring options, which makes it versatile with a clinical deployment and research use. This feature is not only a diagnostic function of AI but a continuous decision support.

Received: Sep 17 2025

International Journal of Applied Mathematics

Volume 39 No. 1s 2026,

ISSN: 1311-1728 (printed version); ISSN: 1314-8060 (on-line version)

Table 1. Summary of literature review on AI-based BC detection methods

Ref	Year	Model	Dataset Type	CAD	Data base	Post Data-review
[32]	2023	Faster R-CNN + U-Net	Ultrasound	No	No	No
[33]	2025	Faster R-CNN + U-Net	Mammography	No	No	No
[34]	2024	Mask R-CNN + Detectron2	MRI	No	No	No
[35]	2024	Faster R-CNN + Group Convolution	Mammography	No	No	No
[36]	2021	Faster R-CNN	Histopathology	No	No	No
[37]	2024	YOLO	Mammography	No	No	No
[38]	2022	YOLO + Transformer	Mammography	No	No	No
[39]	2021	YOLO	Mammography	No	No	No
[40]	2025	YOLO-based	Mammography	No	No	No
[41]	2023	Hybrid: GoogLeNet + AlexNet	Mammography	No	No	No
[42]	2022	AlexNet	Mammography	No	No	No
[43]	2024	DenseNet201 + AlexNet	Mammography	No	No	No
[44]	2024	VGG16	Thermography	No	No	No
[45]	2021	VGG16	Mammography	No	No	No
[46]	2024	InceptionV3, VGG16, VGG19	Mammography	No	No	No
[47]	2024	InceptionV3, GoogLeNet	Thermography	No	No	No
[48]	2024	Inception, GoogleNet	Mammography	No	No	No

Received: Sep 17 2025

Volume 39 No. 1s 2026,

ISSN: 1311-1728 (printed version); ISSN: 1314-8060 (on-line version)

[49]	2023	GoogLeNet	Ultrasound	No	No	No
[50]	2022	Inception V3, V4, Modified Inception	Thermography	No	No	No
[51]	2024	GoogLeNet	Ultrasound	No	No	No
[52]	2023	ResNet vs VGG	Histopathology	No	No	No
[53]	2024	Inception-ResNet v2	Ultrasound	No	No	No
[54]	2021	ResNet-based	Unspecified	No	No	No
[55]	2024	ResNet-101	Ultrasound	No	No	No
[56]	2024	3D Inception-ResNet V2 + Grad-CAM	Mammography	No	No	No
[57]	2022	DenseNet	Histopathology	No	No	No
[58]	2022	DenseNet-169	Histopathology	No	No	No
[59]	2025	DenseNet + XAI	Mammography	No	No	No
[60]	2023	DenseNet121 + Hybrid Statistical/Texture Features	Mammography	No	No	No
[61]	2022	Multichannel DenseNet	Mammography	No	No	No
[62]	2021	Transfer Learning	Mammography	No	No	No
[63]	2024	Inception-ResNet + CapsuleNet	Medical Images	No	No	No
[64]	2024	Hybrid Features Fusion Framework	Ultrasound)	No	No	No
[65]	2022	MobileNet + Optimal Region Growing	Mammography	No	No	No
[66]	2024	Hybrid Deep Learning	Mammography	No	No	No

Received: Sep 17 2025

Volume 39 No. 1s 2026,

ISSN: 1311-1728 (printed version); ISSN: 1314-8060 (on-line version)

[67]	2024	Hybrid Pre-trained Models	Mammography	No	No	No
[68]	2025	EfficientNet-B0 + CNN + Bi-LSTM	Mammography	No	No	No
[69]	2024	VGG11 + EfficientNet	Mammography	No	No	No
[70]	2022	EfficientNet	Mammography	No	No	No
[71]	2022	CNN-LSTM	UWB Microwave Imaging	No	No	No
[72]	2025	LSTM + MGTO	Mammography	No	No	No
[73]	2024	Conv1D + LSTM	Unspecified	No	No	No
[74]	2025	Hybrid CNN + LSTM	Mammography	No	No	No
[75]	2022	CNN + LSTM + Random Forest	Mammography	No	No	No
[76]	2025	EfficientNet + GRU	Histopathology	No	No	No
[77]	2022	RNN + GRU	Mammography	No	No	No
[78]	2024	GRU with Attention + CapsNet	Mammography	No	No	No
[79]	2025	Hybrid ViT + GRU	Mammography	No	No	No
[80]	2025	Improved GRU	Mammography	No	No	No
[81]	2025	Bi-RNN	Histopathology	No	No	No
[82]	2025	Hybrid ViT + GRU	Mammography	No	No	No
[83]	2024	Deep Neural	Tabular/Clinical	No	No	No
[84]	2024	DA-CNN, Bi-GRU EfficientNet	Multimodal	No	No	No
[85]	2023	Hybrid Deep Learning Architecture	Mammography	No	No	No

Received: Sep 17 2025

Volume 39 No. 1s 2026,

ISSN: 1311-1728 (printed version); ISSN: 1314-8060 (on-line version)

[86]	2022	Deep Hybrid Architectures	Mammography	No	No	No
[88]	2024	Hybrid CNN & RNN	Mammography	No	No	No
[91]	2025	CNN + RNN	Mammography	No	No	No
[93]	2024	Hybrid CNN-RNN	Thermography	No	No	No
[94]	2021	Feature Fusion + Fractal	Mammography	No	No	No
[95]	2022	TTCNN	Mammography	No	No	No
[96]	2021	Transfer Learning (Various CNNs)	Ultrasound	No	No	No
[97]	2023	Deep BC Net (Custom DL)	Ultrasound	No	No	No
[98]	2021	Deep Learning Model (CNN)	Ultrasound	No	No	No

2. The Proposed Methodology

The proposed BRE-CAD framework follows an end-to-end operational pipeline that integrates data preparation, deep learning–based lesion detection, system-level deployment, and clinical data management, as illustrated in Figure 1. Rather than presenting a purely conceptual workflow, this section outlines the practical implementation stages adopted in this study. The methodology is structured into four interconnected components: (i) data pipeline and preprocessing, (ii) model training and optimization, (iii) system integration and visualization, and (iv) database-driven diagnostic management.

First, a curated subset of 5,304 mammographic images was extracted from the VinDr-Mammo dataset and processed through a dedicated data pipeline. This pipeline includes mass extraction, bounding box annotation, dataset refinement, and partitioning into training (80%), validation (15%), and testing (5%) subsets. These steps ensure consistent data formatting and clinically meaningful supervision for model learning. Second, a Faster Regional Convolutional Neural Network (R-CNN) detection model was employed as the core analytical engine. The model performs hierarchical feature extraction, region proposal generation, and joint classification–localization of suspicious breast lesions. Training and validation were conducted iteratively, with hyperparameter tuning guided by performance metrics to obtain the optimal detection configuration. Third, the trained model was embedded into a graphical user interface that enables real-time and offline mammogram analysis. Detected lesions are visualized with

Received: Sep 17 2025

Volume 39 No. 1s 2026,

ISSN: 1311-1728 (printed version); ISSN: 1314-8060 (on-line version)

confidence scores, allowing clinicians to interactively review model outputs and support diagnostic decision-making.

Finally, an integrated PostgreSQL backend was implemented to store mammographic images, detection results, and diagnostic metadata. This database layer enables secure data persistence, longitudinal patient tracking, and retrospective clinical review. The overall framework is further extended through an IoT-enabled communication layer, allowing remote access and centralized management of diagnostic records. This structured methodology ensures alignment between data processing, model development, and clinical deployment, forming a cohesive pipeline from raw mammographic input to interpretable decision support.

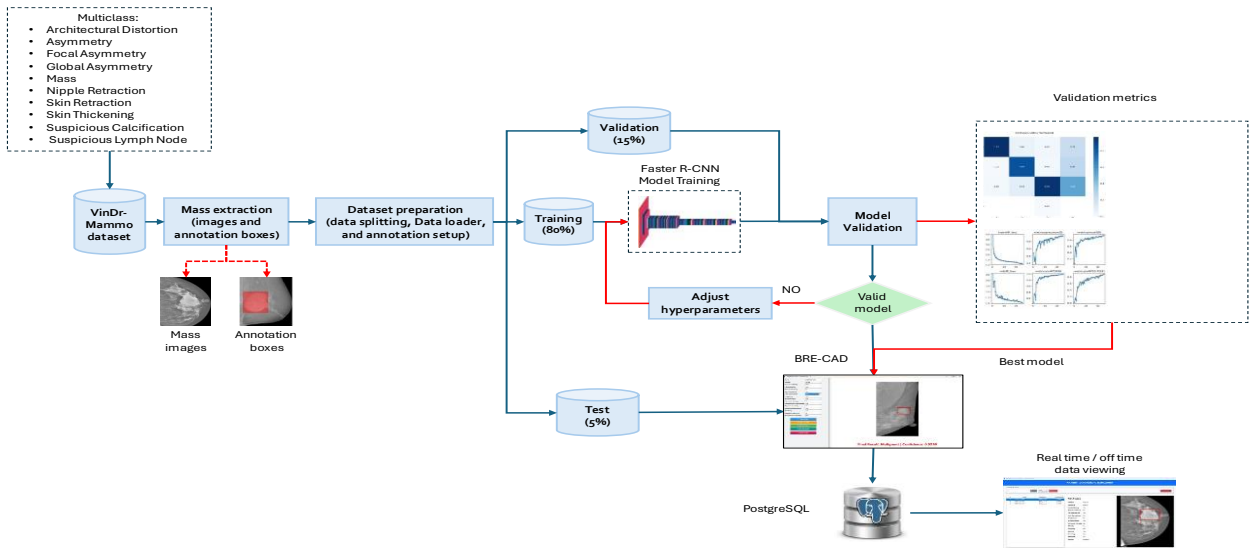

Figure 1. The proposed research methodology

2.1. Data Pipeline and Preprocessing

The data management step is one of the most important steps in BRE-CAD, and it guarantees that the model is being trained on high-quality information that is clinically relevant. It is done by taking advantage of a massive publicly available dataset and applying a specific data mining pipeline that extracts and refines the data. The main source of the data on this research will be the "VinDr-Mammo" dataset a massive and open-source collection of mammograms of the breast cancer screening [113]. This dataset is one of its kind because it is rich in clinical information comprising of: (1) Imaging Data: 20,000 high-resolution Digital Mammography (DM) images in DICOM format. (2) Expert Annotations: Every picture is linked to clinical results, such as the site of abnormalities (bounding boxes) and the evaluation of the density of the breast. (3) Clinical Metadata: The information is classified according to the BI-RADS (Breast Imaging-Reporting and Data System) scaling, which offers a standardized vocabulary of describing the findings in terms of the masses, calcifications, and structural deformities. Figure 2 defines a custom Data Pipeline that was designed to do the customization of the enormous "VinDr-Mammo" dataset to the needs of the BRE-CAD system. It is a pipeline that

Received: Sep 17 2025

Volume 39 No. 1s 2026,

ISSN: 1311-1728 (printed version); ISSN: 1314-8060 (on-line version)

automates the process of converting raw clinical files to a structured training format. It is performed in the following steps: (1) Metadata Parsing: The pipeline is acting upon the CSV files related to the descriptive labels of the whole set of data. (2) Feature Extraction & Filtering: A filtering algorithm was used to search the CSV records and filter out specific attributes that were necessary in tumor detection such as; Image IDs: To match labels with their corresponding mammogram file; Pathology Labels: Filtering cases that are specifically labeled as either Benign or Malignant (Mass); Geometric Coordinates: Extraction of bounding box parameters to pinpoint the precise site of the lesions. (3) Dataset Refinement: This automated extraction refined 5,304 images (1768 malignant, 3536 benign) in a focused set. This made sure that the model training was concentrated on high quality, annotated images of high-quality masses, which minimized noise and enhanced the accuracy of the Faster R-CNN detector. (4) Format Standardization: This is the final part of the pipeline where the metadata extracted is converted to a format recognizable by deep learning frameworks and this conversion ensures it can be effortlessly integrated into the training loop of the model. Figure 3, gives the visual description of the original data set of VinDr-mamo with the multiclass and with cured dataset with mass class to develop the model. The curated dataset was subdivided into three independent subsets in order to assess the predictive power and the reliability of the BRE-CAD system. This split guarantees that the model is trained in an effective manner, and it is strictly tested with unknown data. Table 1 serves as the partitioning, but its detailed description was as follows: (1) Training Set (80%): It was based on this subset that the weights of the Faster R-CNN model were optimized. It comprises a proportional distribution of benign and malignant masses where the network is able to know the various morphological aspects of the breast tumors. (2) Validation Set (15%): This set served as an in-house check in the training phase. It was applied to optimize the hyperparameters (learning rate and number of epochs) and to screen the model against overfitting so that the learning process would be generalized. (3) Testing Set (5%): This set will give the ultimate performance results of the BRE-CAD simulating the system would give in a real-life clinical setting.

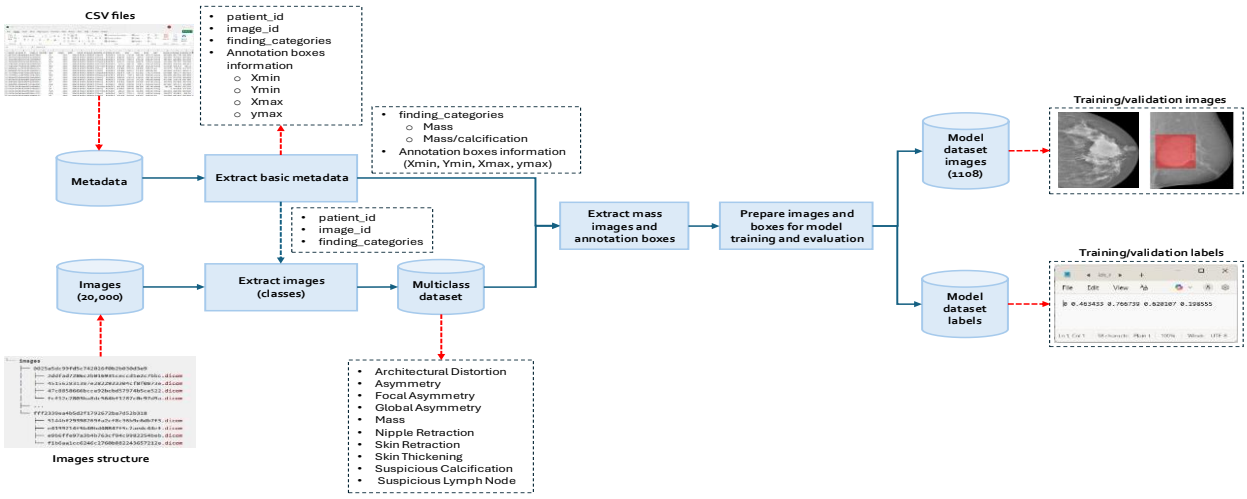

Figure 2. dataset preparation and portioning

Received: Sep 17 2025

International Journal of Applied Mathematics

Volume 39 No. 1s 2026,

ISSN: 1311-1728 (printed version); ISSN: 1314-8060 (on-line version)

Table 1. dataset partitioning

VinDr-mamo dataset (original)	curated dataset (model dataset)	Malignant/ Benign		Dataset portioning
20,000 images (findings, and no findings)	5,304 images 1768 labels	Malignant	1768 images 1768 labels	Training Set (80%)
		Benign	3,536 images 0 labels	Validation Set (15%)
				Testing Set (5%)

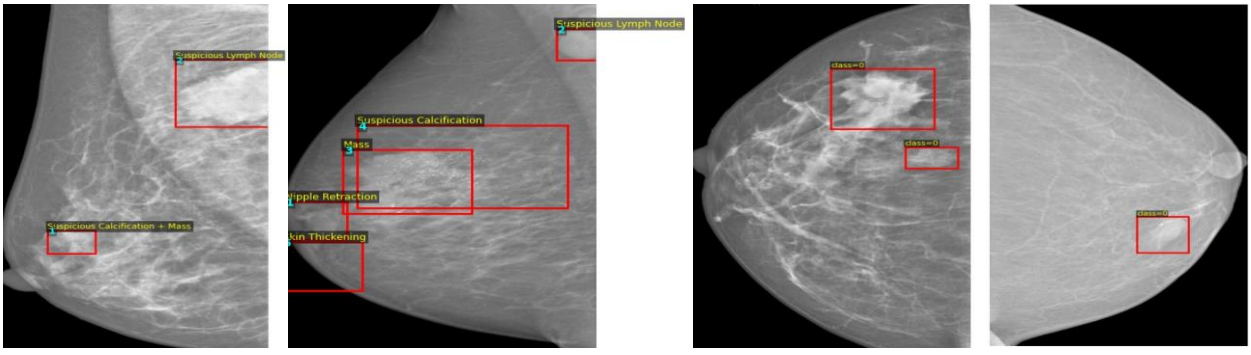

(A) VinDr mamo multiclass dataset

(B) Class 0: mass dataset

Figure 3. (A) multiclass VinDr-mamo dataset visual example, (B) single class (mass) cured dataset visual example

2.2. Model development

The suggested BRE-CAD system is developed based on the Faster R-CNN architecture, a novel and cutting-edge deep learning system of object detection, as it is more robust and accurate in the medical image analysis. The model is shown in the system architecture Figure 4 and it comprises two stages of detection pipeline that is aimed at correctly localizing and classifying breast cancer areas on the mammogram images. This process of detection involves three major steps. To begin with, at the feature extraction phase, a deep convolutional backbone using the ResNet-50 architecture combined with a Feature Pyramid Network (FPN) will be used to obtain hierarchical spatial features of the input mammogram images. The backbone allows the network to identify both the fine-grained low-level features, e.g. edges and intensity changes, and the high-level semantic features connected to abnormal breast tissue. The multi-scale

Received: Sep 17 2025

International Journal of Applied Mathematics

Volume 39 No. 1s 2026,

ISSN: 1311-1728 (printed version); ISSN: 1314-8060 (on-line version)

feature of the FPN also increases the capability of this model to identify the lesions of different sizes.

Mathematically, the input mammogram image is represented as a grayscale tensor [114]:

$$I \epsilon \mathbb{R}^{H \times W} \quad (1)$$

where H and W denote the spatial dimensions of the image. Each convolutional layer inside the backbone computes features responses according to:

$$y_{i,j}^{(k)} = \sum_m \sum_n x_{i+m,j+n} w_{m,n}^{(k)} + b^{(k)} \quad (2)$$

where x represents the input feature map, w the convolution kernel, and b the bias term. The nonlinear activation applied after convolution is the Rectified Linear Unit (ReLU):

$$f(x) = \max(0, x) \quad (3)$$

In the residual blocks of ResNet-50, the transformation is defined as:

$$y = F(x, W) + x \quad (4)$$

where $F(x, W)$ denotes the residual mapping and x is the identity shortcut connection that stabilizes gradient propagation. Within the FPN module, multi-scale feature maps are constructed using a top-down pathway with lateral connections:

$$P_l = Conv(C_l) + UpSample(P_{l+1}) \quad (5)$$

where C_l represents the backbone feature map at level l and P_l denotes the pyramid feature map.

Second, the extracted feature maps are then given to the Region Proposal Network (RPN) which produces a set of candidate regions (anchors) that can harbor tumor tissues. The RPN analyzes every anchor with an objectness rating and initial bounding box regression to differentiate between the foreground and the background. This step greatly narrows down on the search space maintaining high diagnostic relevance regions [115].

The RPN classification (objectness) loss is defined as:

$$L_{cls}^{RPN} = -[p^* \log(p) + (1 - p^*) \log(1 - p)] \quad (6)$$

where p is the predicted probability and p^* is the ground-truth label. Bounding box regression is parameterized relative to anchor coordinates as:

$$t_x = \frac{x - x_a}{w_a}, t_y = \frac{y - y_a}{h_a} \quad (7)$$

$$t_w = \log(\frac{w}{w_a}), t_h = \log(\frac{h}{h_a}) \quad (8)$$

The regression loss is computed using the Smooth L1 function:

$$SmoothL1(x) = \begin{cases} \frac{1}{2}x^2, & |x| < 1 \\ |x| - \frac{1}{2}, & otherwise \end{cases} \quad (9)$$

Received: Sep 17 2025

International Journal of Applied Mathematics
Volume 39 No. 1s 2026,
ISSN: 1311-1728 (printed version); ISSN: 1314-8060 (on-line version)

The total RPN loss is therefore:

$$L_{RPN} = L_{cls}^{RPN} + \lambda L_{reg}^{RPN} \quad (10)$$

Lastly, Region of Interest (RoI) pooling is applied to the proposed regions in the Fast R-CNN head to generate fixed-size feature representations:

$$ROI = Pool(F, r) \quad (11)$$

These representations are then used to perform two tasks in parallel. The first is classification of each region as either Benign or Malignant using the Softmax function:

$$P(c|x) = \frac{e^{z_c}}{\sum_{j=1}^{C} e^{z_i}} \quad (12)$$

The detection classification loss is defined as:

$$L_{cls}^{Det} = -\sum_{c=1}^{C} y_c \log(P(c|x)) \quad (13)$$

The total Faster R-CNN loss used during training becomes:

$$L_{Total} = -L_{RPN} + L_{cls}^{Det} + L_{reg}^{Det} \quad (14)$$

During training, gradient-based optimization updates model parameters according to [116]:

$$\theta_{t+1} = \theta_t + \eta \nabla_\theta L_{Total} \quad (15)$$

Where η is the learning rate and θ denotes the model parameters.

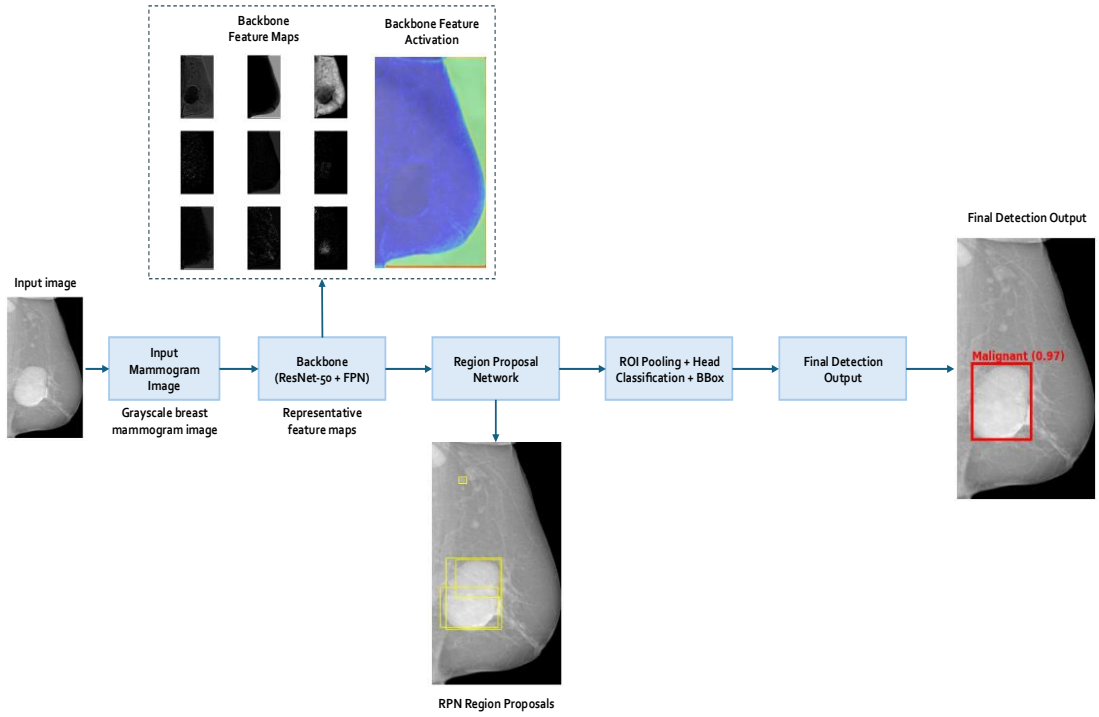

Figure 4. Overview of the BRE-CAD system architecture based on the Faster R-CNN framework.

Received: Sep 17 2025

International Journal of Applied Mathematics

Volume 39 No. 1s 2026,

ISSN: 1311-1728 (printed version); ISSN: 1314-8060 (on-line version)

The training phase was done on a rigorous optimization strategy to guarantee high diagnostic performance and convergence stability. Implementation of the model was based on the PyTorch framework and trained on a CUDA-enabled GPU which facilitates the efficient execution of the computation intensive tensors involved in deep convolutional networks. AdamW optimizer was used because it allows decoupling of the weight decay and gradient update process which offers a better regularization than the standard Adam optimizer and minimizes the chances of overfitting to medical imaging textures. The learning rate was chosen as 1×10^{-4} as it allows keeping the gradient descent stable and avoiding oscillating convergence. The model was trained until 15 epochs, which was also empirically found as the best point where training and validation loss curves stopped reducing. Multi-task loss was introduced in the training, which is the classification loss (log loss over the predicted classes) plus the bounding box regression loss (Smooth L1 loss). At every iteration, gradient-based learning using backpropagation was used to update the model parameters. In order to understand the internal learning behavior in the trained network, backbone intermediate feature maps were extracted and visualized. Through this qualitative analysis, it is apparent that the backbone is useful in paying attention to the salient areas of the mammogram images, especially those with irregular textures and intensity changes that are usually the effect of the malignant tissues. These observations are the confirmation that the Faster R-CNN model gradually converts raw grayscale medical images to meaningful representations that can be used to detect and localize breast cancer effectively.

2.3. The BRE-CAD System pipeline

The BRE-CAD system design is developed on an integrated system that can guarantee diagnostic accuracy, fastness of data transmission and storage. The design consists of three major layers: Processing Layer, IoT and connectivity Layer and the Management Layer. The general architectural design of the system is shown in Figure 5. The input stage of the workflow is the stage where raw mammogram images are received. The Faster R-CNN model is integrated and works on the image to extract essential features which allow localization and classifying of tumors. In addition to diagnosis, the system serves as a gateway where such results are relayed via secured protocols to the cloud which enables the integration of Internet of Things (IoT) to conduct remote monitoring of the patient. The examination interface provided in Figure 6 is used as the direct interface with the system. This interface is made as a Data Aggregation Point. After the detection has been performed: (1) The results (classification, confidence scores, and tumor coordinates) are transformed into a digital format (structured). (2) This information is then fed into an "IoT Module" integrated into the software to update the patient record in real-time. (3) The interface enables the clinician to initiate the commands of sending/ saving, which synchronizes the local findings with the central PostgreSQL database through the internet. In order to maintain continuity of care, the system has a special module that reviews data that is stored as shown in Figure 7. This element of the design can be used as a Management Dashboard, where healthcare providers can: (1) Access past medical records in the database. (2) Compare the present screenings against the past to track down the tumor development or response to the treatment. (3) Check the integrity of information being sent over the network and all the detection done during the examination stage must be properly

Received: Sep 17 2025

Volume 39 No. 1s 2026,

ISSN: 1311-1728 (printed version); ISSN: 1314-8060 (on-line version)

archived. The data structure of BRE-CAD is based on the conversion of the graphical output to the description metadata. Upon detection of a tumor, the system sends a packet that has the Patient ID, Timestamp and Diagnostic Result. This information is encrypted and transmitted through internet to the database server. The IoT-based workflow enables sharing of data with specialists in various geographical areas easily which is a fundamental requirement of smart healthcare applications of the present times.

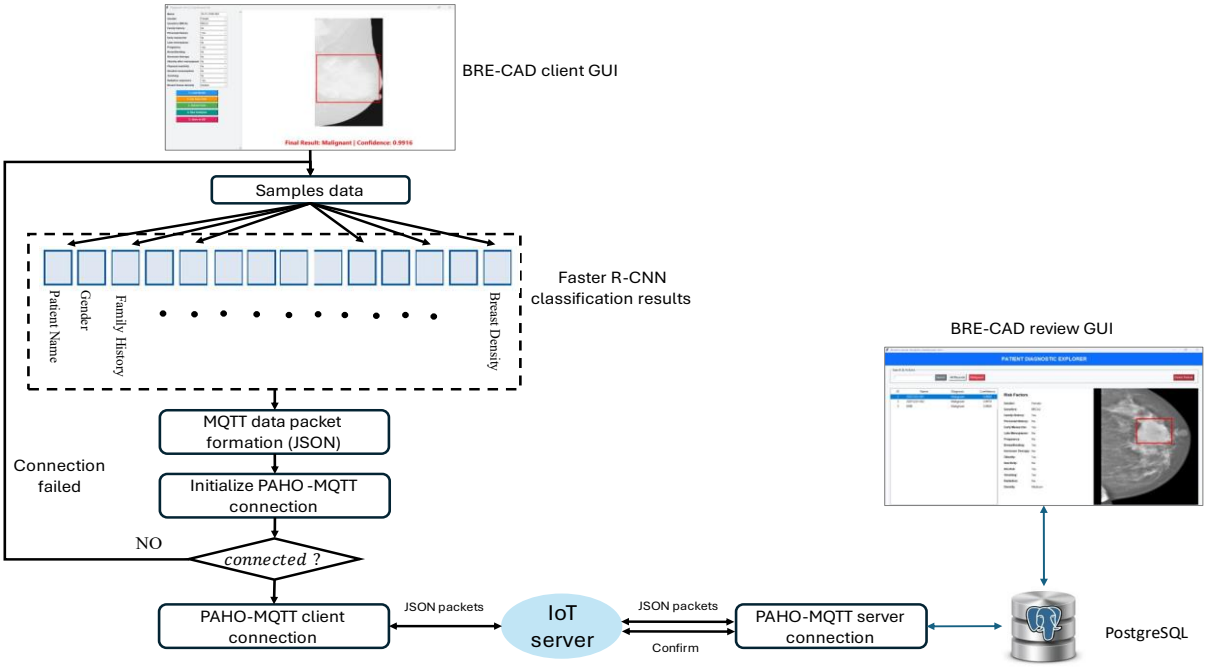

Figure 5. The overall architectural framework of the BRE-CAD system, illustrating the end-to-end data flow from image acquisition to cloud storage.

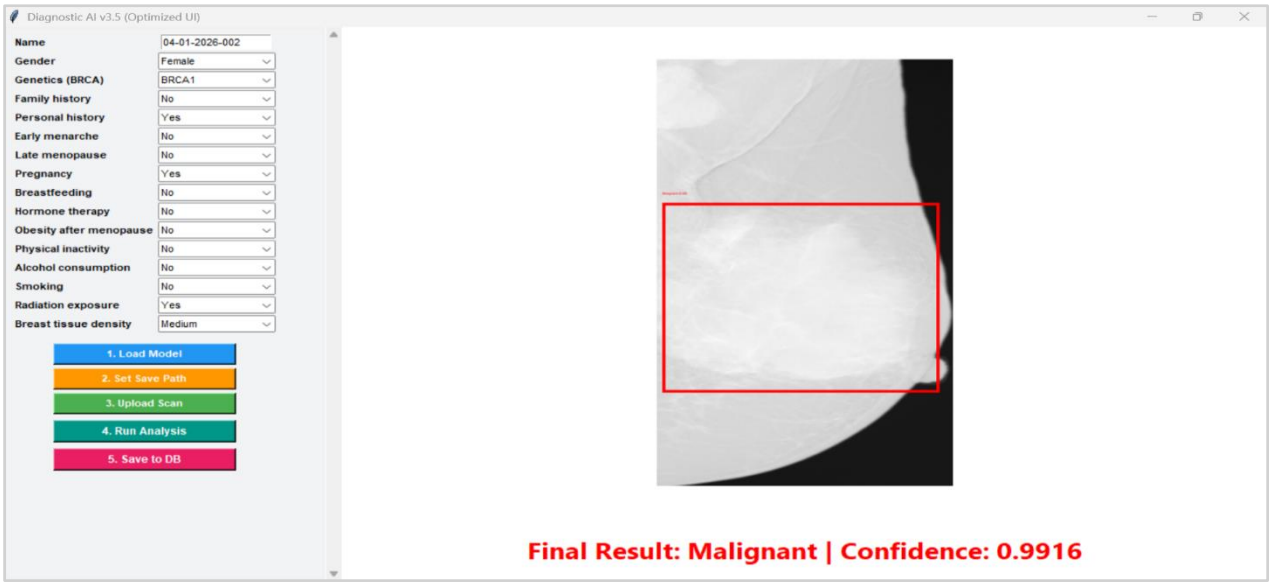

Figure 6. The BRE-CAD examination interface showing real-time tumor detection and the integrated data transmission controls.

Received: Sep 17 2025

International Journal of Applied Mathematics

Volume 39 No. 1s 2026,

ISSN: 1311-1728 (printed version); ISSN: 1314-8060 (on-line version)

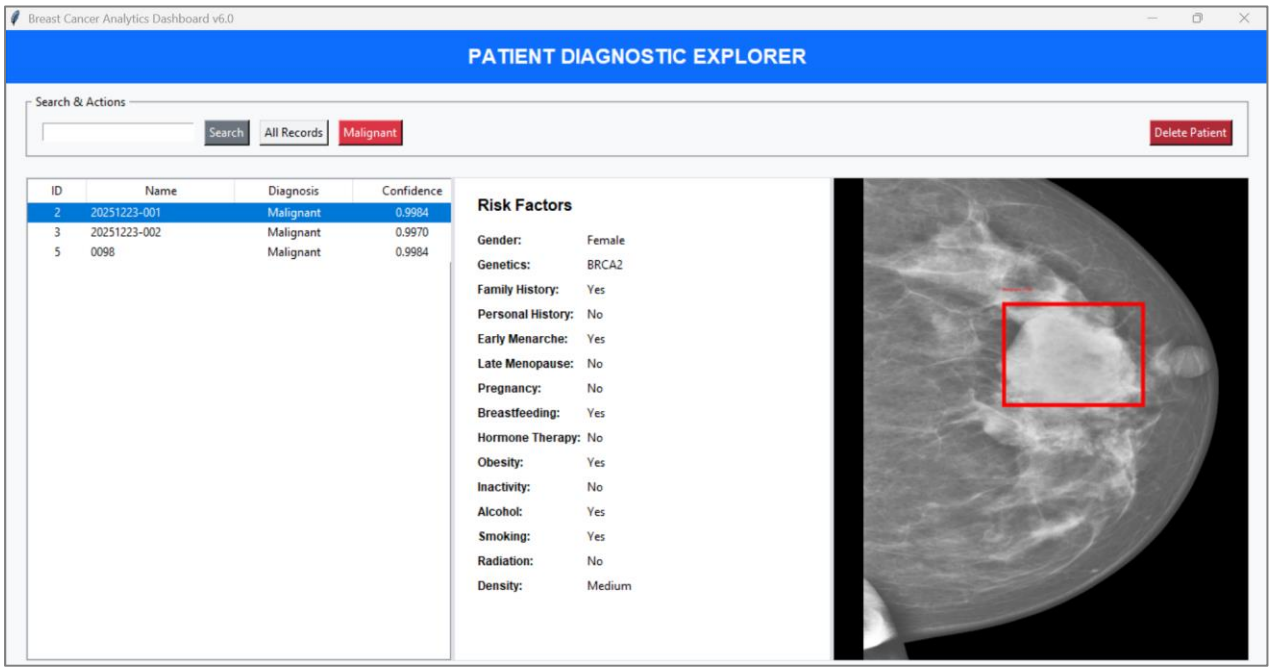

Figure 7. The data review and management module for accessing archived patient records and historical diagnostic reports.

2.4. The IoT Module

The proposed BRE-CAD system is incorporated into an IoT-based architecture to make it feasible to implement into the real-world setting and ensure its clinical applicability (Figure 8). The design is such that it turns the deep learning detection model into a distributed, network-sensitive diagnostic platform that has the capability to service the modern healthcare setting. The architecture helps to facilitate smooth communication among imaging equipment, diagnostic programs, centralized servers, and healthcare workers to make it very scalable, reachable, and efficient. The proposed framework has X-ray images of the mammography data collected at the first phase where standard digital mammography equipment is utilized and then the data is transferred to the BRE-CAD client software. The client application is the local interface that allows submitting the images and visualizing them, which would enable the healthcare facilities with limited computational resources to access the sophisticated diagnostic features. After acquisition, mammographic images are safely sent to the IoT server which acts as the central processing and communication node of the system through the Internet. When an image is sent, the IoT server uses the trained deep learning detection model to process the mammogram and detect any suspicious areas that could be evidence of possible breast cancer. The model generates the coordinates of a bounding box and confidence scores associated with the latter, and that is subsequently sent back to the client software in near real time. This two-way communication enables clinicians to quickly check the findings of the detections without having to install on-site high-performance computing hardware to support diagnostics and telemedicine applications, thus. Diagnostic data such as mammographic images, detection results, patient metadata as well as system logs are all persistently stored in a centralized

Received: Sep 17 2025

Volume 39 No. 1s 2026,

ISSN: 1311-1728 (printed version); ISSN: 1314-8060 (on-line version)

postgreSQL database. Necessary outputs in this database layer include longitudinal monitoring of patients, facilitating retrospective clinical analysis, and making diagnoses traceable. Moreover, a centralized repository of data makes it easier to improve the system in the future, both through retraining of the model, performance audit and large scale statistical assessment, which are needed to ensure the diagnostic reliability as time progresses. BRE-CAD server software is a specialized graphical user interface, which enables radiologists and other medical personnel to view identified tumor areas, check confidences, as well as, conduct clinical verification. More importantly, the system has an approach of human-in the loop design philosophy, when artificial intelligence supports but does not substitute medical knowledge. Clinicians are not restricted to diagnostic choices and can provide feedback or remedial measures to the system, which further reinforces trust, accountability, and clinical safety. The proposed BRE-CAD system will help generate the necessary link between the algorithmic and practical research and clinical implementation of the study by adding an IoT-enabled infrastructure to the deep learning-based breast cancer detection. The architecture facilitates the scalable functionality of many healthcare institutions, access to the diagnostic services remotely and offers a secure centralized platform to manage medical data. Therefore, the system is a major leap to smart, networked and clinically implementable computer-aided diagnosis systems in breast cancer screening and early detection.

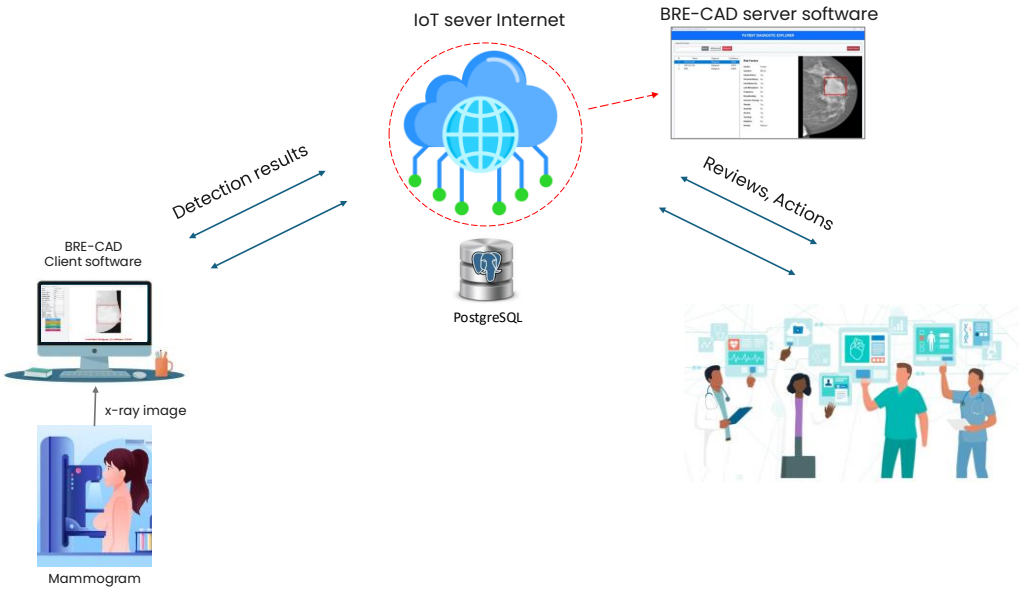

Figure 8. IoT-enabled architecture of the proposed BRE-CAD system illustrating the interaction between mammographic imaging devices, client software, cloud-based detection server, centralized database, and clinical review layer.

3. Experimental results

To quantitatively assess the diagnostic performance of the proposed BRE-CAD system, multiple evaluation metrics were employed to capture both lesion localization accuracy and classification effectiveness. Since breast cancer screening involves simultaneous detection of suspicious regions and pathological categorization, a comprehensive set of metrics was adopted to provide a multidimensional performance analysis. The accuracy of the bounding box

Received: Sep 17 2025

International Journal of Applied Mathematics

Volume 39 No. 1s 2026,

ISSN: 1311-1728 (printed version); ISSN: 1314-8060 (on-line version)

localization is measured using the IoU metric. It calculates the overlap between the predicted bounding box (B_p) and the ground truth box (B_{gt}):

$$\text{IoU} = \frac{Area(B_p \cap B_{gt})}{Area(B_p \cup B_{gt})} \quad (16)$$

A threshold (typically 0.5) is set to determine whether a detection is a True Positive (TP) or a False Positive (FP). Precision Measures the accuracy of the positive predictions (how many detected masses were actually tumors).

$$\text{Precision} = \frac{TP}{TP+FP} \quad (17)$$

Recall Measures the ability of the system to find all relevant cases (how many of the actual tumors were detected). This is the most critical metric in cancer screening.

$$\text{Recall} = \frac{TP}{TP+FN} \quad (18)$$

F1-Score is the harmonic mean of Precision and Recall, providing a single score that balances both metrics, especially useful if there is a class imbalance.

$$\text{F1} = 2\frac{\text{Precision} \times \text{Recall}}{\text{Precision} + \text{Recall}} \quad (19)$$

The mAP is the gold standard for evaluating CNN models. It calculates the "average accuracy" for each of the breast cancer categories at different levels of "recall," and then takes the overall average. This metric provides a comprehensive view of the model's stability and its ability to distinguish between benign and malignant under different lighting and confidence conditions.

$$\text{mAP} = \frac{1}{N}\sum_{i=1}^{N} AP_i \quad (20)$$

where $P_i$denotes the average precision of class iii, and N represents the total number of evaluated classes.

The experimental findings prove the learning and detection skill of the proposed BRE-CAD system on a Faster R-CNN framework. According to Figure 9, the training loss significantly decreases very fast and at a steady rate in the initial epochs and then gradually approaches the limit after around 6 th epoch. This practice reflects a good optimization and proves that the model manages to extract the discriminative features with help of mammography’s and does not show any signs of divergence or unreliable training. Figure 10 shows the trend of precision, recall, and F1-score on the validation set in terms of image-level classification. The model has a trade-off balance between precision and recall, and the F1-score levels out at 0.67. It is important to note that recall values always surpass the precision which is a desirable trait in clinical screening situations since it is more focused on the reduction of false negative and minimizes chances of false alarms to detect cancer-suspected cases. Figure 11, the confusion matrix, gives more details about the diagnostic behavior of the system. The model is right in its identification that a large percentage of healthy cases (735 true negatives) and it manages to identify a considerable number of cancer-suspected images (309 true positives). This is also true although there are some misclassifications that still occur especially the false positives but

Received: Sep 17 2025

Volume 39 No. 1s 2026,

ISSN: 1311-1728 (printed version); ISSN: 1314-8060 (on-line version)

this is what is expected of a medical decision-support system, which involves being conservative with sensitivity, rather than being precise with specificity. Altogether, the proposed BRE-CAD model has a number of significant advantages, including the steady convergence of training, the regularity of performance improvement, the beneficial effect of the clinics, and the ability to distinguish between normal and cancer-suspect mammograms. These findings affirm the development of the suggested deep learning model into an IoT-based BRE-CAD setting as a support system to help radiologists, specifically in preliminary screening and decision support as opposed to conclusive diagnosis.

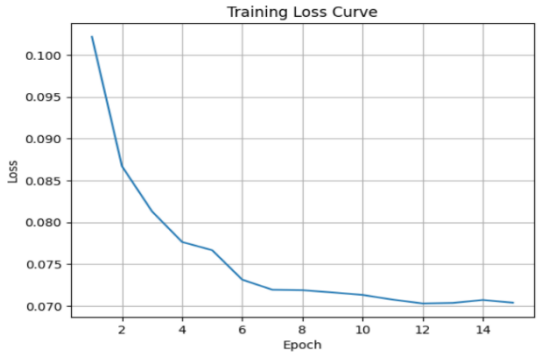

Figure 9. Training loss curve of the Faster R-CNN-based BRE-CAD model across training epochs.

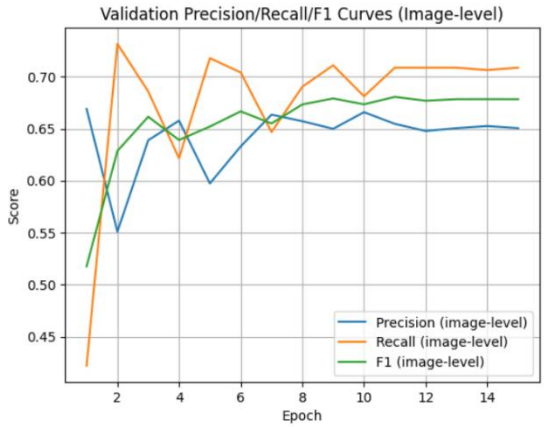

Figure 10. Image-level precision, recall, and F1-score trends on the validation dataset

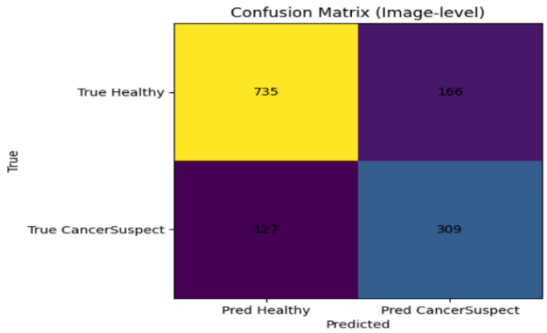

Figure 11. Confusion matrix illustrating image-level classification results for healthy and cancer-suspected mammograms.

Received: Sep 17 2025

International Journal of Applied Mathematics

Volume 39 No. 1s 2026,

ISSN: 1311-1728 (printed version); ISSN: 1314-8060 (on-line version)

Even though the received performance scores are average in contrast to fully monitored state-of-the-art breast cancer detection systems, one should put these results into perspective of the limitations of the used data and experimental design. First, there are only a relatively small number of available annotated samples with accurate bounding boxes which has a direct influence on the learning performance of region-based object detectors including Faster R-CNN. Second, mammographic lesions tend to have low contrast, indistinct visual features, and indistinct borders, thus, being naturally challenging to localize even to the trained radiology expert, and, by extension, deep learning models. Moreover, the mammographic scans that are used in the current study are resized instead of high-resolution mammographic scans. Although the need to resize along with making certain computational feasibility and deep learning framework compatibility is inevitable, it is bound to cause partial loss of fine-grained texture and structural details that play a crucial role in correctly localizing lesions. Irrespective of these complications, the suggested BRE-CAD model exhibits the stable convergence, stable performance enhancement and clinically desirable recall habits, which prove that the model effectively learns useful representations, instead of being biased towards learning shallow patterns. The given system is more focused on robustness and practical deployability in the environment based on the IoT within a clinical setting when compared to methods that are trained on fully balanced, high-resolution datasets with dense annotations. Thus, the obtained outcomes must be considered an effective baseline of a real-life screening helping, instead of a highest-level diagnostic performance. The next research will aim at adding more finer-resolution inputs, more annotated samples, and discuss multi-scale and attention-based architectures to add further to the recognition precision.

A qualitative analysis was done on a randomly selected 5% of the test data to further analyze the practical behavior of the proposed BRE-CAD system. This analysis is intended to be used in addition to the quantitative measures to be able to gain graphical understanding of the way the model makes decisions and see possible weaknesses and limitations of the model in the real-life situation of screening. The identified samples were segregated as three representative groups as shown in Figures 12,13,14. The former, as demonstrated in Figure 12, is the first category which represents cancer-suspected mammograms that the system identifies correctly. The model was effective in such instances where it found abnormal regions with bounding boxes and high confidence scores were attributed. The identified areas visually match clinical suspect tissue patterns, and the model has the capability to learn meaningful lesion-related information even in low image resolution and low annotation levels.

Received: Sep 17 2025

International Journal of Applied Mathematics
Volume 39 No. 1s 2026,
ISSN: 1311-1728 (printed version); ISSN: 1314-8060 (on-line version)

Figure 12. Correctly detected cancer-suspected mammograms from the 5% test subset, showing accurate localization and high confidence scores.

The second category, as shown in Figure 13, comprises of healthy mammograms that were correctly diagnosed as normal. In these samples, the proposed system had no bounding-box detections and always gave almost zero confidence. This pattern shows that the model is successful at suppressing false alarms and points out that the model is able to differentiate between normal and pathological patterns of the breast anatomy, including dense tissue and complicated anatomical anomalies in the images. The third category, which is depicted in Figure 14, is healthy mammograms which were falsely identified as cancer-suspect (false positives). Whereas in such cases, the model was able to identify localized areas and score moderate confidence. Two factors may be used to explain this phenomenon. To begin with, the dataset documentation makes it clear that not all the images that were marked as healthy have been annotated exhaustively to find subtle or ambiguous abnormalities, and thus it is reasonable to assume that some of the regions that are identified might be unmarked or borderline results. Second, the inherent drawbacks of the detection model, as well as the visual complexity of mammographic images, the presence of overlapping tissues and dissimilar textures, may result in conservative predictions that are more sensitive than specific. Notably, these false positive identifications do not suggest erratic or random model behavior. Rather, related confidence scores indicate that the system can distinguish high levels of suspicion and uncertain areas. Clinically speaking, such sensitivity-attracted conduct is more desirable, since it decreases the opportunity of overlooking any possible abnormalities, and promotes further expert analysis of this data instead of automated conclusions. In general, qualitative analysis of the 5% test subset validates that the proposed BRE-CAD system demonstrates clinically interpretable behavior and screening-based behavior. The model is reliable in identifying obvious cases of cancer, suppressing cases of normal images, and warning about suspicious cases with ambiguous cases. These results support the appropriateness of proposed system as a decision-support system. in an IoT-based breast cancer screening system.

Received: Sep 17 2025

International Journal of Applied Mathematics
Volume 39 No. 1s 2026,
ISSN: 1311-1728 (printed version); ISSN: 1314-8060 (on-line version)

Figure 13. Healthy mammograms correctly classified as normal, illustrating the absence of detections and near-zero confidence scores.

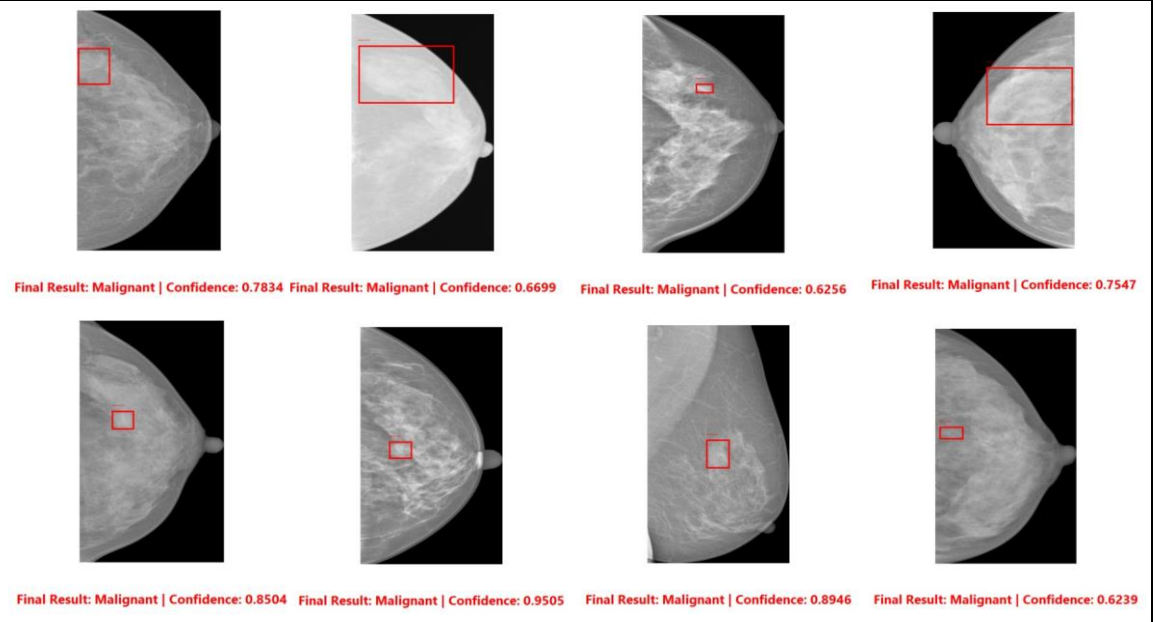

Figure 14. Healthy mammograms misclassified as cancer-suspected, demonstrating false positive detections due to ambiguous tissue patterns and potential dataset annotation limitations.

In this paper, a computer-aided diagnosis (CAD) system known as BRE-CAD was proposed, which is IoT enabled and is used to detect breast cancer via a Faster R-CNN-based deep learning model. It was trained and tested on a selected subset of the VinDr-Mammo dataset of 5,304 mammographic images (1,768 malignant, 3,536 benign) and a realistic data partitioning

Received: Sep 17 2025

Volume 39 No. 1s 2026,

ISSN: 1311-1728 (printed version); ISSN: 1314-8060 (on-line version)

plan of 80 percent training, 15 percent validation and 5 percent testing to mimic conditions in the real world. The quantitative assessment revealed that learning behavior remained stable and converged consistently as indicated by training loss curve, which dropped sharply within the first few epochs but became stable after the sixth one. Evaluation on the validation and test sets at image-level provided an equal performance, with F1-score of around 0.67, and a recall always greater than precision, which is clinically desirable in screening uses. The confusion matrix also validated that the system is conservative in its diagnostic approach as it was able to reach the goal of 735 true negatives and 309 true positives with the controlled number of false positives to reduce the number of missed cases with suspected cancer. In addition to numerical measures, qualitative analysis on a random 5 per cent test subset gave more insight into the practice behavior of the system. The BRE-CAD system was seen to have a high confidence score of localizing suspicious areas of the cancer in a reliable manner, a high success rate in suppressing any unknowns found in normal mammograms, and a careful approach to raising any uncertain cases. These observations point to the appropriateness of the system as a decision support tool, as opposed to a diagnostic authority of its own.

Conclusions and future work

This paper presented BRE-CAD, a unified breast cancer computer-aided diagnosis system that fills the gap between the research in the field of deep learning and its clinical implementation. BRE-CAD is built as a full end-to-end diagnostic and data management system, unlike most of the current literature that uses an algorithmic model alone, as the framework includes a Faster R-CNN model and a graphical user interface, as well as a PostgreSQL database, which can be easily extended to a real-world screening setting. As the results of the experiment show, despite the performance metrics already being moderate, as compared to full-supervision and high-resolution benchmark systems, the proposed model has a number of clinically relevant strengths. They are stable training convergence, reliability of learning behavior, and diagnostic tendency that is recall oriented; this is especially important in breast cancer screening because it minimizes the cases of the false-negative. The confusion matrix as well as the trends of precision-recall has shown that the system focuses on sensitivity, which is in line with clinical safety. A qualitative study performed on 5 percent of the test sample also confirms the soundness of the proposed method. Identified cancer-suspected cases that were correctly identified in the localization of lesions showed high confidence and correctly identified healthy cases also exhibited good suppressing false alarms. The cases that were misclassified as healthy mainly were linked to the uncertainty of the patterns of tissues and moderate confidence ratings. Notably, one can also point to model limitations as well as incompleteness of the annotations that are documented in the dataset, which is also recognized in the original source of VinDr-Mammo. This observation supports the conclusion that the behavior of the model is conservative but not chaotic. All in all, BRE-CAD is an effective and interpretable screening-based CAD system helping radiologists identify the suspicious areas, sort diagnostic data, and review the cases within the longitudinal context. The system would be better placed as a support clinical tool that supplements the early detection processes as opposed to substituting professional judgment. Although the proposed system of BRE-CAD indicates a good

Received: Sep 17 2025

Volume 39 No. 1s 2026,

ISSN: 1311-1728 (printed version); ISSN: 1314-8060 (on-line version)

performance, there are a number of directions to be improved. To start with, the future research will involve adding more data to be labeled and improved, specifically adding more accurately labeled bounding boxes and annotations reviewed by experts in order to decrease the number of ambiguous cases (healthy). Second, the high-resolution mammographic inputs will be explored to maintain fine-grained texture and structure of the mammography that are essential in the process of locating fine lesions, particularly micro-masses and low-contrast lesions. This will have the benefit of increasing the accuracy of localization and the confidence of classification. Third, more complicated architectural extensions, including multi-scale attention, feature fusion, and transformer-based detection head will be considered to enhance sensitivity to small and heterogeneous lesions. Moreover, the use of explainable AI (XAI) methods would allow further building clinical trust through providing visual explanations of model predictions. Lastly, subsequent iterations of BRE-CAD will focus on multi-modal data integration (ultrasound, MRI, structured clinical risk factors) to enhance the strength of diagnosis. The prospective validation of the system scale and the clinician-in-the-loop assessment of the system will also be sought to determine the effects of the system in the actual screening processes and the diagnostic decision-making.

References

[1] J. Kim *et al.*, "Global patterns and trends in breast cancer incidence and mortality across 185 countries," *Nat. Med.*, vol. 31, no. 4, pp. 1154–1162, 2025, doi: 10.1038/s41591-025-03502-3.

[2] A. S. H. Alsheikhly and M. A. Alsheikhly, "A Comprehensive Review of Breast Cancer and the Latest Advancement in Diagnosis and Treatment," in *Latest Research on Breast Cancer - Molecular Insights, Diagnostic Advances and Therapeutic Innovations*, A. C. Monteiro and L. Wang, Eds., Rijeka: IntechOpen, 2025. doi: 10.5772/intechopen.1008946.

[3] H. Almohanna *et al.*, "A comprehensive epidemiological analysis of breast cancer in the Eastern Province of Saudi Arabia," *Sci. Rep.*, vol. 15, no. 1, p. 20816, 2025, doi: 10.1038/s41598-025-05276-7.

[4] P. Ciamarra *et al.*, "Surgical Treatment, Rehabilitative Approaches and Functioning Assessment for Patients Affected by Breast Cancer-Related Lymphedema: A Comprehensive Review," *Medicina 2025, Vol. 61, Page 1327*, vol. 61, no. 8, p. 1327, Jul. 2025, doi: 10.3390/MEDICINA61081327.

[5] R. Singh, S. Tuominen, M. I. Lassenius, M. Auvinen, A. Torstensson, and T. Wiklund, "Real-World Observational Study of Incidence and Outcomes in an HR+/HER2– Early Breast Cancer Population with High-Risk of Recurrence in Finland," *Oncol. Ther.*, vol. 13, no. 1, pp. 185–200, 2025, doi: 10.1007/s40487-024-00324-0.

Received: Sep 17 2025

Volume 39 No. 1s 2026,

ISSN: 1311-1728 (printed version); ISSN: 1314-8060 (on-line version)

[6] S. I. Mohammed, "The Importance of MRI Imaging to Detect Breast Cancer: A Review.," *Rafidain Journal of Science*, vol. 34, no. 1, pp. 110–120, Mar. 2025, doi: 10.33899/RJS.2025.186500.

[7] Y. Cai, F. Dai, Y. Ye, and J. Qian, "The global burden of breast cancer among women of reproductive age: a comprehensive analysis," *Sci. Rep.*, vol. 15, no. 1, p. 9347, 2025, doi: 10.1038/s41598-025-93883-9.

[8] I. Rodrigues *et al.*, "Is Progesterone Receptor a Neglected Feature in Breast Cancer? A Retrospective Study Analysing the Clinicopathological Characteristics of Breast Cancer Based on Progesterone Receptor Status," *Clin. Breast Cancer*, vol. 25, no. 4, pp. e331–e340, 2025, doi: https://doi.org/10.1016/j.clbc.2024.11.018.

[9] J. Subelack, R. Morant, M. Blum, A. Eichenberger, A. Geissler, and D. Ehlig, "Risk factors for interval breast cancer: insights from a decade of a mammography screening program," *Breast Cancer Res. Treat.*, vol. 211, no. 1, pp. 23–33, 2025, doi: 10.1007/s10549-025-07619-4.

[10] Z. Long, Y. Qiu, Z. Long, and Z. Jin, "Epidemiology of breast cancer in Chinese women from 1990 to 2021: a systematic analysis and comparison with the global burden," *BMC Cancer*, vol. 25, no. 1, p. 3, 2025, doi: 10.1186/s12885-024-13336-w.

[11] R. N. Pillai *et al.*, "Economic burden of breast cancer in India, 2000–2021 and forecast to 2030," *Sci. Rep.*, vol. 15, no. 1, p. 1323, 2025, doi: 10.1038/s41598-024-83896-1.

[12] B. An, M. Che, Y. Liu, X. Yang, and Z. Li, "Analysis and comparison of the burden of male breast cancer: differences between the global, China, India, and the United States," *BMC Public Health*, vol. 25, no. 1, p. 2205, 2025, doi: 10.1186/s12889-025-23120-5.

[13] G. Zannini *et al.*, "BRCA1 and BRCA2 mutations testing in prostate cancer: Detection in formalin fixed paraffin embedded (FFPE) and blood samples," *Pathol. Res. Pract.*, vol. 266, p. 155803, Feb. 2025, doi: 10.1016/J.PRP.2024.155803.

[14] H. Park *et al.*, "Prediction of Germline BRCA Mutations in High-Risk Breast Cancer Patients Using Machine Learning with Multiparametric Breast MRI Features," *Sensors 2025, Vol. 25, Page 5500*, vol. 25, no. 17, p. 5500, Sep. 2025, doi: 10.3390/S25175500.

[15] J. Earl, A. Kataki, F. Canzian, E. Costello, D. Campa, and W. Greenhalf, "Targeting pancreatic cancer screening by identification of pathogenic variants of BRCA2/ BRCA1 in healthy individuals who have no known family history of pancreatic

Received: Sep 17 2025

Volume 39 No. 1s 2026,

ISSN: 1311-1728 (printed version); ISSN: 1314-8060 (on-line version)

cancer: The arguments for and against.," *Semin. Cancer Biol.*, vol. 113, pp. 1–8, Aug. 2025, doi: 10.1016/J.SEMCANCER.2025.05.001.

[16] G. Y. Moon *et al.*, "Cell-Free DNA Versus Circulating Tumor Cells: A Pilot Study of Alpha-Fetoprotein Analysis for Diagnosis and Treatment Monitoring in Hepatocellular Carcinoma," *Biosensors (Basel).*, vol. 15, no. 9, p. 579, 2025.

[17] S. Mohammad *et al.*, "Role of circulating tumor DNA and cell-free DNA biomarkers in diagnosis and prognosis of oral cancer - a systematic review," *BMC Oral Health*, vol. 25, no. 1, p. 522, 2025, doi: 10.1186/s12903-025-05898-3.

[18] P. Rigotti *et al.*, "Cell-Free DNA as a Prognostic Biomarker in Oral Carcinogenesis and Oral Squamous Cell Carcinoma: A Translational Perspective," *Cancers 2025, Vol. 17, Page 2366*, vol. 17, no. 14, p. 2366, Jul. 2025, doi: 10.3390/CANCERS17142366.

[19] M. G. Cerdas *et al.*, "Exploring the Evolution of Breast Cancer Imaging: A Review of Conventional and Emerging Modalities," *Cureus*, vol. 17, no. 4, 2025.

[20] N. Salhi, R. Hampson, G. Dobie, and S. Neale, "Optimizing Non-Invasive Early Breast Cancer Screening: A Review of the Role of Tactile Imaging and Ultrasound in Primary Care," 2025.

[21] C. Comparetto and F. Borruto, "Cutting-edge Imaging Breakthroughs for Early Breast Cancer Detection," *Cancer Screening and Prevention*, vol. 4, no. 1, pp. 21–39, 2025.

[22] J. He, N. Liu, and L. Zhao, "New progress in imaging diagnosis and immunotherapy of breast cancer," *Front. Immunol.*, vol. 16, p. 1560257, 2025.

[23] G. Y. Moon *et al.*, "Cell-Free DNA Versus Circulating Tumor Cells: A Pilot Study of Alpha-Fetoprotein Analysis for Diagnosis and Treatment Monitoring in Hepatocellular Carcinoma," *Biosensors (Basel).*, vol. 15, no. 9, p. 579, 2025.

[24] B. Abdikenov *et al.*, "Future of Breast Cancer Diagnosis: A Review of DL and ML Applications and Emerging Trends for Multimodal Data," *IEEE Access*, 2025.

[25] M. A. Wahed, M. Alqaraleh, M. S. Alzboon, and M. S. Al-Batah, "Evaluating AI and Machine Learning Models in Breast Cancer Detection: A Review of Convolutional Neural Networks (CNN) and Global Research Trends," *LatIA*, vol. 3, p. 117, 2025.

[26] A. M. Sharafaddini, K. K. Esfahani, and N. Mansouri, "Deep learning approaches to detect breast cancer: a comprehensive review," *Multimed. Tools Appl.*, vol. 84, no. 21, pp. 24079–24190, 2025.

[27] J. Majidpour and H. Beitollahi, "A Comprehensive Examination of Machine Learning and Deep Learning Approaches for Breast Cancer Detection,

Received: Sep 17 2025

Volume 39 No. 1s 2026,

ISSN: 1311-1728 (printed version); ISSN: 1314-8060 (on-line version)

Classification, Segmentation, Augmentation, and Feature Selection," *Archives of Computational Methods in Engineering*, pp. 1–32, 2025.

[28] M. A. Rahman *et al.*, "Advancements in Breast Cancer Detection: A Review of Global Trends, Risk Factors, Imaging Modalities, Machine Learning, and Deep Learning Approaches," *BioMedInformatics*, vol. 5, no. 3, p. 46, 2025.

[29] R. D. Ghongade and D. G. Wakde, "Computer-aided diagnosis system for breast cancer using RF classifier," *Proceedings of the 2017 International Conference on Wireless Communications, Signal Processing and Networking, WiSPNET 2017*, vol. 2018-January, pp. 1068–1072, Jul. 2017, doi: 10.1109/WiSPNET.2017.8299926.

[30] V. Ponomaryov, "Computer-aided detection system based on PCA/SVM for diagnosis of breast cancer lesions," *CHILECON 2015 - 2015 IEEE Chilean Conference on Electrical, Electronics Engineering, Information and Communication Technologies, Proceedings of IEEE Chilecon 2015*, pp. 429–436, Feb. 2016, doi: 10.1109/Chilecon.2015.7400413.

[31] R. M. Masoud, R. M. A. Bakir, M. S. Saraya, and S. M. Ayyad, "BREAST-CAD: A Computer-Aided Diagnosis System for Breast Cancer Detection Using Machine Learning," *Technologies 2025, Vol. 13,* vol. 13, no. 7, Jun. 2025, doi: 10.3390/technologies13070268.

[32] K. Oh, S. E. Lee, and E.-K. Kim, "3-D breast nodule detection on automated breast ultrasound using faster region-based convolutional neural networks and U-Net," *Sci. Rep.*, vol. 13, no. 1, p. 22625, 2023, doi: 10.1038/s41598-023-49794-8.

[33] S. D. Y, A. G, P. V, A. K, A. K. P. V, and R. K. L. Makesh, "Breast-FRUNET: Automated Breast Cancer Classification Using X-Ray Images with Faster R-CNN and U-Net," in *2025 International Conference on Computing Technologies (ICOCT)*, 2025, pp. 1–8. doi: 10.1109/ICOCT64433.2025.11118812.

[34] C. H. Salh and A. M. Ali, "Automatic detection of breast cancer for mastectomy based on MRI images using Mask R-CNN and Detectron2 models," *Neural Comput. Appl.*, vol. 36, no. 6, pp. 3017–3035, 2024, doi: 10.1007/s00521-023-09237-x.

[35] Z. Sani, R. Prasad, and E. K. M. Hashim, "Breast Cancer Detection in Mammography using Faster Region Convolutional Neural Networks and Group Convolution," *IETE J. Res.*, vol. 70, no. 9, pp. 7379–7395, Sep. 2024, doi: 10.1080/03772063.2024.2352643.

[36] P. Harrison and K. Park, "Tumor Detection In Breast Histopathological Images Using Faster R-CNN," in *2021 International Symposium on Medical Robotics (ISMR)*, 2021, pp. 1–7. doi: 10.1109/ISMR48346.2021.9661483.

Received: Sep 17 2025

Volume 39 No. 1s 2026,

ISSN: 1311-1728 (printed version); ISSN: 1314-8060 (on-line version)

[37] F. Prinzi, M. Insalaco, A. Orlando, S. Gaglio, and S. Vitabile, "A Yolo-Based Model for Breast Cancer Detection in Mammograms," *Cognit. Comput.*, vol. 16, no. 1, pp. 107–120, 2024, doi: 10.1007/s12559-023-10189-6.

[38] Y. Su, Q. Liu, W. Xie, and P. Hu, "YOLO-LOGO: A transformer-based YOLO segmentation model for breast mass detection and segmentation in digital mammograms," *Comput. Methods Programs Biomed.*, vol. 221, p. 106903, 2022, doi: https://doi.org/10.1016/j.cmpb.2022.106903.

[39] G. H. Aly, M. Marey, S. A. El-Sayed, and M. F. Tolba, "YOLO Based Breast Masses Detection and Classification in Full-Field Digital Mammograms," *Comput. Methods Programs Biomed.*, vol. 200, p. 105823, 2021, doi: https://doi.org/10.1016/j.cmpb.2020.105823.

[40] B. K. Karaca Aydemir, Z. Telatar, S. Güney, and B. Dengiz, "Detecting and classifying breast masses via YOLO-based deep learning," *Neural Comput. Appl.*, vol. 37, no. 17, pp. 11555–11582, 2025, doi: 10.1007/s00521-025-11153-1.

[41] S. R, N. M, V. B, R. N, and S. E, "An Improved Fusion Model from GoogLeNet and AlexNet to Predict Breast Cancer using Deep Learning," in *2023 International Conference on System, Computation, Automation and Networking (ICSCAN)*, 2023, pp. 1–4. doi: 10.1109/ICSCAN58655.2023.10395210.

[42] S. S. Boudouh and M. Bouakkaz, "Breast Cancer: Using Deep Transfer Learning Techniques AlexNet Convolutional Neural Network For Breast Tumor Detection in Mammography Images," in *2022 7th International Conference on Image and Signal Processing and their Applications (ISPA)*, 2022, pp. 1–7. doi: 10.1109/ISPA54004.2022.9786351.

[43] N. E. Benhassine, A. Boukaache, and D. Boudjehem, "Breast cancer image classification using DenseNet201 and AlexNet based deep transfer learning," in *Proceedings of the International Conference on Emerging Intelligent Systems for Sustainable Development (ICEIS 2024)*, Atlantis Press, 2024, pp. 129–143. doi: 10.2991/978-94-6463-496-9_11.

[44] F. Ahmed, M. Rahman, S. Akter Shukhy, A. Mahmud Sisir, I. Alam Rafi, and R. K. Khan, "Breast Cancer Detection with VGG16: A Deep Learning Approach with Thermographic Imaging," *Breast Cancer Detection with Vgg16: A Deep Learning Approach with Thermographic Imaging*, 2024.

[45] S. Montaha *et al.*, "BreastNet18: a high accuracy fine-tuned VGG16 model evaluated using ablation study for diagnosing breast cancer from enhanced mammography images," *Biology (Basel).*, vol. 10, no. 12, p. 1347, 2021.

[46] K. Kansal and S. Sharma, "Predictive Deep Learning: An Analysis of Inception V3, VGG16, and VGG19 Models for Breast Cancer Detection," in *Advanced*

Received: Sep 17 2025

Volume 39 No. 1s 2026,

ISSN: 1311-1728 (printed version); ISSN: 1314-8060 (on-line version)

Computing, D. Garg, J. J. P. C. Rodrigues, S. K. Gupta, X. Cheng, P. Sarao, and G. S. Patel, Eds., Cham: Springer Nature Switzerland, 2024, pp. 347–357.

[47] R. Jalloul, H. K. Chethan, and R. Alkhatib, "Non-Invasive Breast Cancer Screening: Leveraging InceptionV3 and GoogLeNet for Thermal Image Analysis," in *2024 13th International Conference on Computer Technologies and Development (TechDev)*, IEEE, 2024, pp. 21–26.

[48] W. S. Admass, Y. Y. Munaye, and A. O. Salau, "Integration of feature enhancement technique in Google inception network for breast cancer detection and classification," *J. Big Data*, vol. 11, no. 1, p. 78, 2024.

[49] S.-H. Chen, Y.-L. Wu, C.-Y. Pan, L.-Y. Lian, and Q.-C. Su, "Breast ultrasound image classification and physiological assessment based on GoogLeNet," *J. Radiat. Res. Appl. Sci.*, vol. 16, no. 3, p. 100628, 2023.

[50] M. A. S. Al Husaini, M. H. Habaebi, T. S. Gunawan, M. R. Islam, E. A. A. Elsheikh, and F. M. Suliman, "Thermal-based early breast cancer detection using inception V3, inception V4 and modified inception MV4," *Neural Comput. Appl.*, vol. 34, no. 1, pp. 333–348, 2022.

[51] J. Wang *et al.*, "Using the GoogLeNet deep-learning model to distinguish between benign and malignant breast masses based on conventional ultrasound: a systematic review and meta-analysis," *Quant. Imaging Med. Surg.*, vol. 14, no. 10, p. 7111, 2024.

[52] A. Kanavos and P. Mylonas, "Deep learning analysis of histopathology images for breast cancer detection: A comparative study of resnet and VGG architectures," in *2023 18th International Workshop on Semantic and Social Media Adaptation & Personalization (SMAP) 18th International Workshop on Semantic and Social Media Adaptation & Personalization (SMAP 2023)*, IEEE, 2023, pp. 1–6.

[53] T. L. Nikmah, R. M. Syafei, D. N. Anisa, E. Juanara, and Z. Mahrus, "Inception ResNet v2 for Early Detection of Breast Cancer in Ultrasound Images," *Journal of Information System Exploration and Research*, vol. 2, no. 2, 2024.

[54] Z. Zheng, H. Zhang, X. Li, S. Liu, and Y. Teng, "Resnet-based model for cancer detection," in *2021 IEEE International Conference on Consumer Electronics and Computer Engineering (ICCECE)*, IEEE, 2021, pp. 325–328.

[55] A. C. Yadav, M. H. Kolekar, and M. K. Zope, "ResNet-101 Empowered Deep Learning for Breast Cancer Ultrasound Image Classification.," in *BIOSTEC (1)*, 2024, pp. 763–769.

[56] F. M. Talaat, S. A. Gamel, R. M. El-Balka, M. Shehata, and H. ZainEldin, "Grad-CAM enabled breast cancer classification with a 3D inception-ResNet V2: Empowering radiologists with explainable insights," *Cancers (Basel).*, vol. 16, no. 21, p. 3668, 2024.

Received: Sep 17 2025

Volume 39 No. 1s 2026,

ISSN: 1311-1728 (printed version); ISSN: 1314-8060 (on-line version)

[57] M. A. Wakili *et al.*, "Classification of breast cancer histopathological images using DenseNet and transfer learning," *Comput. Intell. Neurosci.*, vol. 2022, no. 1, p. 8904768, 2022.

[58] A. Vulli, P. N. Srinivasu, M. S. K. Sashank, J. Shafi, J. Choi, and M. F. Ijaz, "Fine-tuned DenseNet-169 for breast cancer metastasis prediction using FastAI and 1-cycle policy," *Sensors*, vol. 22, no. 8, p. 2988, 2022.

[59] M. A. Talukder, "An improved XAI-based DenseNet model for breast cancer detection using reconstruction and fine-tuning," *Results in Engineering*, vol. 26, p. 104802, 2025.

[60] G. Hiremath, J. A. Mathew, and N. K. Boraiah, "Hybrid Statistical and Texture Features with DenseNet 121 for Breast Cancer Classification.," *International Journal of Intelligent Engineering & Systems*, vol. 16, no. 2, 2023.

[61] S. D. Pawar *et al.*, "Multichannel DenseNet architecture for classification of mammographic breast density for breast cancer detection," *Front. Public Health*, vol. 10, p. 885212, 2022.

[62] A. Saber, M. Sakr, O. M. Abo-Seida, A. Keshk, and H. Chen, "A novel deep-learning model for automatic detection and classification of breast cancer using the transfer-learning technique," *IEEe Access*, vol. 9, pp. 71194–71209, 2021.

[63] E. Sadeghnezhad and S. Salem, "InceptionCapsule: Inception-Resnet and CapsuleNet with self-attention for medical image Classification," *arXiv preprint arXiv:2402.02274*, 2024.

[64] M. Alhajlah, "A hybrid features fusion-based framework for classification of breast micronodules using ultrasonography," *BMC Med. Imaging*, vol. 24, no. 1, p. 253, 2024.

[65] J. Dafni Rose, K. VijayaKumar, L. Singh, and S. K. Sharma, "Computer-aided diagnosis for breast cancer detection and classification using optimal region growing segmentation with MobileNet model," *Concurrent Engineering*, vol. 30, no. 2, pp. 181–189, 2022.

[66] V. Anitha, M. Subramaniam, and A. A. Roseline, "Improved breast cancer classification approach using hybrid deep learning strategies for tumor segmentation," *Sens. Imaging*, vol. 25, no. 1, p. 31, 2024.

[67] S. Zarif, H. Abdulkader, I. Elaraby, A. Alharbi, W. S. Elkilani, and P. Pławiak, "Using hybrid pre-trained models for breast cancer detection," *PLoS One*, vol. 19, no. 1, p. e0296912, 2024.

[68] U. K. Lilhore *et al.*, "Hybrid convolutional neural network and bi-LSTM model with EfficientNet-B0 for high-accuracy breast cancer detection and classification," *Sci. Rep.*, vol. 15, no. 1, p. 12082, 2025.

Received: Sep 17 2025

Volume 39 No. 1s 2026,

ISSN: 1311-1728 (printed version); ISSN: 1314-8060 (on-line version)

[69] M. D. Souza, G. A. Prabhu, V. Kumara, and K. M. Chaithra, "EarlyNet: a novel transfer learning approach with VGG11 and EfficientNet for early-stage breast cancer detection," *International Journal of System Assurance Engineering and Management*, vol. 15, no. 8, pp. 4018–4031, 2024.

[70] W. Tasya, S. Sa'idah, B. Hidayat, and F. Nurfajar, "Breast cancer detection using convolutional neural network with EfficientNet architecture," in *2022 IEEE Asia Pacific Conference on Wireless and Mobile (APWiMob)*, IEEE, 2022, pp. 1–6.

[71] M. Lu, X. Xiao, Y. Pang, G. Liu, and H. Lu, "Detection and localization of breast cancer using UWB microwave technology and CNN-LSTM framework," *IEEE Trans. Microw. Theory Tech.*, vol. 70, no. 11, pp. 5085–5094, 2022.

[72] D. Umamaheswari, M. Kannan, I. P. S. Mary, D. J. Rozario, P. M. Savitha, and B. Manimekala, "LSTM-MGTO: a novel early breast cancer detection using long short term memory based modified gorilla troops optimization algorithm," *Network Modeling Analysis in Health Informatics and Bioinformatics*, vol. 14, no. 1, p. 17, 2025.

[73] M. Rastogi, M. Vijarania, N. Goel, A. Agrawal, C. N. Biamba, and C. Iwendi, "Conv1D-LSTM: Autonomous Breast Cancer Detection Using a One-Dimensional Convolutional Neural Network with Long Short-Term Memory," *IEEE Access*, 2024.

[74] M. Kaddes, Y. M. Ayid, A. M. Elshewey, and Y. Fouad, "Breast cancer classification based on hybrid CNN with LSTM model," *Sci. Rep.*, vol. 15, no. 1, p. 4409, 2025.

[75] A. Begum, V. Dhilip Kumar, J. Asghar, D. Hemalatha, and G. Arulkumaran, "A combined deep CNN: LSTM with a random forest approach for breast cancer diagnosis," *Complexity*, vol. 2022, no. 1, p. 9299621, 2022.

[76] M. Pradeepa, B. Sharmila, and M. Nirmala, "A hybrid deep learning model EfficientNet with GRU for breast cancer detection from histopathology images," *Sci. Rep.*, vol. 15, no. 1, p. 24633, 2025.

[77] N. Routray, S. K. Rout, and B. Sahu, "Breast cancer prediction using deep learning technique RNN and GRU," in *2022 Second International Conference on Computer Science, Engineering and Applications (ICCSEA)*, IEEE, 2022, pp. 1–5.

[78] M. G. Maheswari, K. Karthigadevi, and G. E. Rani, "A novel breast cancer detection system from mammographic images using a hyperparameter tuned gated recurrent unit with attention included capsnet," *J. Biomol. Struct. Dyn.*, pp. 1–14, 2024.

[79] M. J. Zobair, M. A. Rahman, M. S. Hossain, N. Khan, M. A. A. K. Akash, and M. H. I. Bijoy, "A Hybrid ViT-GRU Model for Breast Cancer Detection: Addressing

Received: Sep 17 2025

Volume 39 No. 1s 2026,

ISSN: 1311-1728 (printed version); ISSN: 1314-8060 (on-line version)

Class Imbalance Challenges," in *2025 International Conference on Electrical, Computer and Communication Engineering (ECCE)*, IEEE, 2025, pp. 1–7.

[80] T. PB and D. R. S. VENI, "A NOVEL APPROACH FOR BREAST CANCER PREDICTION USING IMPROVED GATED RECURRENT UNIT," *J. Theor. Appl. Inf. Technol.*, vol. 103, no. 9, 2025.

[81] R. B. Chikkala *et al.*, "Enhancing Breast Cancer Diagnosis With Bidirectional Recurrent Neural Networks: A Novel Approach for Histopathological Image Multi-Classification," *IEEE Access*, 2025.

[82] M. J. Zobair, M. A. Rahman, M. S. Hossain, N. Khan, M. A. A. K. Akash, and M. H. I. Bijoy, "A Hybrid ViT-GRU Model for Breast Cancer Detection: Addressing Class Imbalance Challenges," in *2025 International Conference on Electrical, Computer and Communication Engineering (ECCE)*, IEEE, 2025, pp. 1–7.

[83] V. Bai, "Breast cancer recurrence prediction with deep neural network and feature optimization.," *Automatika: Journal for Control, Measurement, Electronics, Computing & Communications*, vol. 65, no. 1, 2024.

[84] A. Thazhayamkotath Mana Subramanian, A. S. Menon, V. Reghunath, J. J. Nair, A. Kalathiparambil Asokakumar, and N. Jayagopal, "Evolution of Hybrid Multi-modal Action Recognition: From DA-CNN+ Bi-GRU to EfficientNet-CNN-ViT," in *International Conference on Pattern Recognition*, Springer, 2024, pp. 339–350.

[85] R. S. Raaj, "Breast cancer detection and diagnosis using hybrid deep learning architecture," *Biomed. Signal Process. Control*, vol. 82, p. 104558, 2023, doi: https://doi.org/10.1016/j.bspc.2022.104558.

[86] H. Zerouaoui and A. Idri, "Deep hybrid architectures for binary classification of medical breast cancer images," *Biomed. Signal Process. Control*, vol. 71, p. 103226, 2022, doi: https://doi.org/10.1016/j.bspc.2021.103226.

[87] P. M. Bala, S. Priyadharshini, S. Usharani, and A. Balachandar, "Hybrid Approach of CNN & RNN for Breast Cancer Detection and Segmentation," in *2024 Third International Conference on Smart Technologies and Systems for Next Generation Computing (ICSTSN)*, 2024, pp. 1–6. doi: 10.1109/ICSTSN61422.2024.10670832.

[88] M. Anitha, C. R. Prasad, and A. R. Sekhar, "Breast Cancer Detection Using CNN and RNN," in *2025 6th International Conference for Emerging Technology (INCET)*, 2025, pp. 1–7. doi: 10.1109/INCET64471.2025.11140855.

[89] A. Munguía-Siu, I. Vergara, and J. H. Espinoza-Rodríguez, "The use of hybrid CNN-RNN deep learning models to discriminate tumor tissue in dynamic breast thermography," *J. Imaging*, vol. 10, no. 12, p. 329, 2024.

Received: Sep 17 2025

Volume 39 No. 1s 2026,

ISSN: 1311-1728 (printed version); ISSN: 1314-8060 (on-line version)

[90] A. Sahu, P. K. Das, and S. Meher, "Recent advancements in machine learning and deep learning-based breast cancer detection using mammograms," *Physica Medica*, vol. 114, p. 103138, 2023, doi: https://doi.org/10.1016/j.ejmp.2023.103138.

[91] D. A. Zebari *et al.*, "Breast cancer detection using mammogram images with improved multi-fractal dimension approach and feature fusion," *Applied Sciences*, vol. 11, no. 24, p. 12122, 2021.

[92] J. H. Yoon *et al.*, "Standalone AI for breast cancer detection at screening digital mammography and digital breast tomosynthesis: a systematic review and meta-analysis," *Radiology*, vol. 307, no. 5, p. e222639, 2023.

[93] K. Dembrower, A. Crippa, E. Colón, M. Eklund, and F. Strand, "Artificial intelligence for breast cancer detection in screening mammography in Sweden: a prospective, population-based, paired-reader, non-inferiority study," *Lancet Digit. Health*, vol. 5, no. 10, pp. e703–e711, 2023.

[94] S. Maqsood, R. Damaševičius, and R. Maskeliūnas, "TTCNN: A breast cancer detection and classification towards computer-aided diagnosis using digital mammography in early stages," *Applied Sciences*, vol. 12, no. 7, p. 3273, 2022.

[95] M. Larsen *et al.*, "Performance of an artificial intelligence system for breast cancer detection on screening mammograms from BreastScreen Norway," *Radiol. Artif. Intell.*, vol. 6, no. 3, p. e230375, 2024.

[96] G. Ayana, K. Dese, and S. Choe, "Transfer learning in breast cancer diagnoses via ultrasound imaging," *Cancers (Basel).*, vol. 13, no. 4, p. 738, 2021.

[97] A. Raza, N. Ullah, J. A. Khan, M. Assam, A. Guzzo, and H. Aljuaid, "DeepBreastCancerNet: A novel deep learning model for breast cancer detection using ultrasound images," *Applied Sciences*, vol. 13, no. 4, p. 2082, 2023.

[98] X. Zhang *et al.*, "Evaluating the accuracy of breast cancer and molecular subtype diagnosis by ultrasound image deep learning model," *Front. Oncol.*, vol. 11, p. 623506, 2021.

[99] N. Aristokli, I. Polycarpou, S. C. Themistocleous, D. Sophocleous, and I. Mamais, "Comparison of the diagnostic performance of Magnetic Resonance Imaging (MRI), ultrasound and mammography for detection of breast cancer based on tumor type, breast density and patient's history: A review," *Radiography*, vol. 28, no. 3, pp. 848–856, 2022.

[100] M. Salim *et al.*, "AI-based selection of individuals for supplemental MRI in population-based breast cancer screening: the randomized ScreenTrustMRI trial," *Nat. Med.*, vol. 30, no. 9, pp. 2623–2630, 2024.

Received: Sep 17 2025

Volume 39 No. 1s 2026,

ISSN: 1311-1728 (printed version); ISSN: 1314-8060 (on-line version)

[101] R. Adam, K. Dell'Aquila, L. Hodges, T. Maldjian, and T. Q. Duong, "Deep learning applications to breast cancer detection by magnetic resonance imaging: a literature review," *Breast Cancer Research*, vol. 25, no. 1, p. 87, 2023.

[102] J. Witowski *et al.*, "Improving breast cancer diagnostics with deep learning for MRI," *Sci. Transl. Med.*, vol. 14, no. 664, p. eabo4802, 2022.

[103] N. Aristokli, I. Polycarpou, S. C. Themistocleous, D. Sophocleous, and I. Mamais, "Comparison of the diagnostic performance of Magnetic Resonance Imaging (MRI), ultrasound and mammography for detection of breast cancer based on tumor type, breast density and patient's history: A review," *Radiography*, vol. 28, no. 3, pp. 848–856, 2022.

[104] D. Wekking, M. Porcu, P. De Silva, L. Saba, M. Scartozzi, and C. Solinas, "Breast MRI: clinical indications, recommendations, and future applications in breast cancer diagnosis," *Curr. Oncol. Rep.*, vol. 25, no. 4, pp. 257–267, 2023.

[105] M. B. Lawson *et al.*, "Comparative performance of contrast-enhanced mammography, abbreviated breast MRI, and standard breast MRI for breast cancer screening," *Radiology*, vol. 308, no. 2, p. e230576, 2023.

[106] M. Daniaux *et al.*, "Preoperative staging by multimodal imaging in newly diagnosed breast cancer: diagnostic performance of contrast-enhanced spectral mammography compared to conventional mammography, ultrasound, and MRI," *Eur. J. Radiol.*, vol. 163, p. 110838, 2023.

[107] B. Dołęga-Kozierowski *et al.*, "Multimodality imaging in lobular breast cancer: differences in mammography, ultrasound, and MRI in the assessment of local tumor extent and correlation with molecular characteristics," *Front. Oncol.*, vol. 12, p. 855519, 2022.

[108] E. A. Abeelh and Z. AbuAbeileh, "Comparative effectiveness of mammography, ultrasound, and MRI in the detection of breast carcinoma in dense breast tissue: a systematic review," *Cureus*, vol. 16, no. 4, 2024.

[109] Y. E. Kim, J. H. Cha, H. H. Kim, H. J. Shin, E. Y. Chae, and W. J. Choi, "The accuracy of mammography, ultrasound, and magnetic resonance imaging for the measurement of invasive breast cancer with extensive intraductal components," *Clin. Breast Cancer*, vol. 23, no. 1, pp. 45–53, 2023.

[110] N. Al-Azzam and I. Shatnawi, "Comparing supervised and semi-supervised machine learning models on diagnosing breast cancer," *Annals of Medicine and Surgery*, vol. 62, pp. 53–64, 2021.

[111] S. Sharmin, T. Ahammad, M. A. Talukder, and P. Ghose, "A hybrid dependable deep feature extraction and ensemble-based machine learning approach for breast cancer detection," *IEEE Access*, vol. 11, pp. 87694–87708, 2023.

Received: Sep 17 2025

Volume 39 No. 1s 2026,

ISSN: 1311-1728 (printed version); ISSN: 1314-8060 (on-line version)

[112] M. T. Mustapha, D. U. Ozsahin, I. Ozsahin, and B. Uzun, "Breast cancer screening based on supervised learning and multi-criteria decision-making," *Diagnostics*, vol. 12, no. 6, p. 1326, 2022.

[113] "VinDr-Mammo: A large-scale benchmark dataset for computer-aided detection and diagnosis in full-field digital mammography v1.0.0." Accessed: Feb. 02, 2026. [Online]. Available: https://physionet-org.translate.goog/content/vindr-mammo/1.0.0/?_x_tr_sl=en&_x_tr_tl=ar&_x_tr_hl=ar&_x_tr_pto=tc

[114] S. Gholinavaz, N. saeedi, and S. S. Gharehveran, "Robustness analysis of YOLO and faster R-CNN for object detection in realistic weather scenarios with noise augmentation," *Scientific Reports 2025 15:1*, vol. 15, no. 1, pp. 44888-, Dec. 2025, doi: 10.1038/s41598-025-28737-5.

[115] A. Magdy, M. S. Moustafa, H. M. Ebied, and M. F. Tolba, "Lightweight faster R-CNN for object detection in optical remote sensing images," *Scientific Reports 2025 15:1*, vol. 15, no. 1, pp. 16163-, May 2025, doi: 10.1038/s41598-025-99242-y.

[116] N. Dong, L. Ericsson, Y. Yang, A. Leonardis, and S. McDonagh, "Label-efficient object detection via region proposal network pre-training," *Neurocomputing*, vol. 577, p. 127376, Apr. 2024, doi: 10.1016/j.neucom.2024.127376.

Received: Sep 17 2025